# Nrf2 overexpression increases risk of high tumor mutation burden in acute myeloid leukemia through inhibiting MSH2

**Ping Liu**
Affiliated Hospital of Guiyang Medical University
**Dan Ma**
Affiliated Hospital of Guiyang Medical University
**Ping Wang**
Affiliated Hospital of Guiyang Medical University
**Chengyun Pan**
Affiliated Hospital of Guiyang Medical University
**Qin Fang**
Affiliated Hospital of Guiyang Medical University
**Jishi Wang** ( wjsxyk0825@163.com )
Affiliated Hospital of Guiyang Medical University

**Research**

**Keywords:** Nuclear factor erythroid 2-related factor 2, MSH2, DNA mismatch repair, Tumor mutation burden, JNK/c-Jun, Acute myeloid leukemia

**Posted Date:** September 1st, 2020

**DOI:** https://doi.org/10.21203/rs.3.rs-66229/v1

# Nrf2 overexpression increases risk of high tumor mutation burden in acute myeloid leukemia through inhibiting MSH2

Ping Liu[1, 2], Dan Ma[1], Ping Wang[1], Chengyun Pan[1, 2], Qin Fang[3], Jishi Wang[1, 4*]

1 Department of Hematology, Affiliated Hospital of Guizhou Medical University, Guizhou Province Institute of Hematology, Guizhou Province Laboratory of Hematopoietic Stem Cell Transplantation Centre, Guiyang, 550004, China.

2 Basic Medical College, Guizhou Medical University, Guiyang, 550001, China.

3 Department of Pharmacy, Affiliated Hospital of Guizhou Medical University, Guiyang, 550004, China

4 National Clinical Research Center for Hematologic Diseases, the First Affiliated Hospital of Soochow University, Jiangsu, 215006, China.

## Abstract

**Background**: Nuclear factor erythroid 2-related factor 2 (Nrf2, also called NFE2L2) has been shown to play a pivotal role in preventing cancer cells from being affected by chemotherapy. Gene mutation is a crucial reason of chemotherapy-resistance in acute myeloid leukemia (AML). However, the relationship between Nrf2 and tumor mutation burden and its mechanism in regulating chemotherapy-resistance remains unclear.

**Methods**: The whole-exome sequencing analysis were used to measure tumor mutation. RNA sequencing, Oncomine, qRT-PCR, Western blotting and immunocytochemistry were employed to detect differences in genes and proteins. The KEGG pathway enrichment analysis and GeneMANIN were performed pathway analysis. Functional assays, such as annexin V/PI, Hoechst33342 staining and DCFH were performed to examine the apoptosis and reactive oxygen species (ROS) of AML cells in vitro. Subcutaneous xenograft model was established to investigate in vivo growth.

**Results**: Nrf2 expression was associated with tumor mutation burden in AML. Patients with Nrf2 overexpression had higher frequency of gene mutation and drug resistance.

Nrf2 overexpression protected the AML cells from apoptosis induced by cytarabine in vitro and increased the risk of gene mutant drug resistance in vivo. Furthermore, Nrf2 overexpression inhibited MSH2 protein expression, which caused DNA mismatch repair (MMR) deficiency. Mechanistically, the inhibition of MSH2 by Nrf2 was in a ROS-independent manner. Further studies showed that an increased activation of JNK/c-Jun signaling in Nrf2 overexpression cells, which inhibited the expression of MSH2 protein.

**Conclusions**: Our findings provided evidence that high Nrf2 expression inhibited MSH2 expression, caused MMR deficiency and increased the tumor mutation burden, which can induce gene instability-dependent drug resistance in AML. This study demonstrates the reason why the high Nrf2 expression leads to the increase of gene mutation frequency in AML, and provides a new strategy for clinical practice.

**Keywords:** Nuclear factor erythroid 2-related factor 2, MSH2, DNA mismatch repair, Tumor mutation burden, JNK/c-Jun, Acute myeloid leukemia

## Background

Acute myeloid leukemia (AML) is a malignant tumor of myeloid progenitor cells characterized by immature myeloid cell proliferation and bone marrow failure. Standard “7+3” induction therapy, which combines a nucleoside analogue such as cytarabine (Ara-C) for 7 days with an anthracycline for 3 days, is highly effective in killing leukemic cells in AML. Despite the fact that the majority of AML patients achieve complete remission after chemotherapy, the 5-year overall survival is very poor, especially in patients over 60 years of age [1, 2]. Most patients die of their disease due to either refractory (initial resistance to chemotherapy) or relapsed AML [3]. Therefore,

the resistance of leukemia cells to chemotherapy drugs becomes the main obstacle in the treatment of AML.

Many hypotheses have been proposed to explain therapeutic resistance. Resistance to anticancer therapy can arise via different mechanisms in AML, including the persistence of leukemic stem cells [4], increased antioxidant defense systems [5], altered expression of drug influx and efflux transporters [6], evasion of cell death [7], and epigenetic mechanisms including DNA methylation and histone modification [8, 9]. Tumor microenvironment is also involved in the development of acquired resistance to chemotherapeutics [10]. In addition, tumor cells are insensitive to chemotherapeutic drugs, due to the presence of complex abnormal karyotypes of chromosomes and gene mutations [11]. Therefore, exploring the molecular mechanism of gene instability-dependent drug resistance is a significant strategy to overcome the resistance.

Nuclear factor-erythroid 2-related factor 2 (Nrf2, also called NFE2L2) is one of the cancer cell survival pathways that is implicated in protecting cancer cells from apoptosis [12]. Nrf2 functions to change the sensitivity of the tumor cells environment to oxidants and electrophiles by stimulating the transcriptional activation of cytoprotective genes [13]. And Nrf2 can reduce the apoptosis of the tumor cells and increase drug resistance [14]. Conversely, inhibition of Nrf2 signaling enhances apoptosis in response to oxidative insults [15]. There are many studies showing elevated expression of Nrf2 in various types of tumors such as head and neck [16], gastric [17], non-small cell lung [18], esophageal squamous cell carcinoma [19], breast [20], gallbladder [21] and ovarian [22] cancer. Upon oxidative stress, Nrf2 signaling is activated and protects tumor cells from cell death by upregulating ROS scavenging enzymes that counterbalance 0production [23]. Nrf2 protects tumor cells from death by

cooperating with other pathways, which plays a role in apoptosis regulation. For example, the tumor suppressor p53 inhibits Nrf2 signaling by down-regulating the expression of Nrf2 target genes, and induces cell apoptosis [24]. In addition, mutant p53 can upregulate Nrf2 expression at the transcriptional level, resulting in anti-apoptosis and chemotherapy resistance [25]. Importantly, p62 is another Nrf2 target, which is upregulated and phosphorylated, thus causing Nrf2 translocation to the nucleus, thereby inhibiting apoptosis [26]. Moreover, Nrf2 binds the ARE sequence on its promoter to up-regulate the Bcl-2 expression, which prevents cellular apoptosis and induces drug resistance [27]. These studies indicate that Nrf2 inhibits apoptosis and confers resistance through different pathways, which play a crucial role in tumor suvival and chemotherapy-resistance.

However, the existing reports are mostly limited to the effect of high Nrf2 expression on gene instability-independent drug resistance, and there are few reports of Nrf2 participating in the regulation of gene instability. In early study, we compared the differentially expressed genes in the two groups of AML patients with high or low Nrf2 expression by transcriptome sequencing (RNAseq), and found that the high Nrf2 expression had a significant inhibitory effect on DNA Mismatch repair (MMR) pathway, which was closely related to gene instability. Genomic instability plays an important role in the development of cancer [28]. The MMR is vital for the maintenance of genomic stability of human cells. Biochemical and genetic studies in eukaryotes have found several MMR genes, including MSH2, MLH1, MSH6, PMS2, POLD2, RFC4 and so on [29, 30]. Normally, cells are equipped with DNA damage response pathways and damage to DNA is detected and repaired [31]. Defective mismatch repair cells exhibit a higher frequency of mutation in both coding and noncoding microsatellite sequences. MMR deficiency leading to microsatellite instability (MSI) has been

recognized as a distinct tumorigenesis pathway [32]. Additionally, DNA repair defects are associated with the development of resistance to chemotherapeutics, in both solid tumors and haematological malignancies [33, 34].

In this study, we sought to investigate the role of Nrf2 in AML gene instability-dependent drug resistance. We found that Nrf2 was significantly up-regulated in AML with high tumor mutation burden and drug resistance. Further analysis revealed that Nrf2 overexpression inhibited MSH2, thereby promoting chemotherapy resistance of AML cells both in vitro and in vivo. Mechanistically, the role of Nrf2 in causing DNA MMR deficiency was achieved by regulating JNK/c-Jun signaling.

## Materials and methods

### Patients' specimens and cell lines

We collected 33 bone marrow specimens of AML patients from September 2018 to May 2019 at the Affiliated Hospital of Guizhou Medical University. Details of clinical information is provided in Table 1. Prior patient consent and approval from the Institutional Research Ethics Committee were obtained.

Human AML cell lines Kasumi-1 and THP-1 were obtained from Guizhou Province Laboratory of Haematopoietic Stem Cell Transplantation Center. The cell lines were cultured in RPMI-1640 medium supplemented with 10% fetal bovine serum, penicillin (100 units/mL) and streptomycin (100 mg/mL) at 37 °C in a humidified atmosphere with 5% $CO_2$.

### Reagents and antibodies

Cytarabine (Ara-C), and SP600125 (a JNK inhibitor) were purchased from MCE, China. N-acetylcysteine (NAC), a reactive oxygen species (ROS) scavenger, was purchased from Coolaber (Beiijng, China). Fetal bovine serum and RPMI 1640 medium were obtained from Gibco (Carlsbad, CA, USA). Western blot analysis was performed using anti-JNK (#9252), anti-phospho-JNK (#4668), anti-phospho-c-Jun (#2361), and anti-c-Jun (#9165) antibodies purchased from Cell Signaling Technology (Danvers, MA, USA). Anti-MSH2 (15520-1-AP) and anti-β-actin (20536-1-AP) antibodies were obtained from Proteintech Group Co., Ltd. (Wuhan, China). Anti-Nrf2 (K106685P) antibody was obtained from solarbio (Beijing, China).

**Lentiviral transduction**

Human Nrf2 overexpression clone lentiviral particle (L-Nrf2) and human Nrf2-silencing RNA (si-Nrf2) were purchased from Genechem Co., Ltd. (Shanghai, China). Transfection of Nrf2 was performed using manufacturer's instructions. Cells (THP1 and Kasumi-1) respectively transfected with empty vector (EV) were used as controls. After expansion and maintenance in RPMI-1640 medium supplemented with 10% FBS for 5 days, stable THP-1 and Kasumi-1 cell lines expressing L-Nrf2 or si-Nrf2 were selected by puromycin (1.5μg/ml and 2μg/ml respectively).

**Quantitative real-time PCR (qRT-PCR)**

Total RNAs from cells were extracted using Trizol reagent (Invitrogen, Carlsbad, CA, USA) according to the manufacturer's instructions. Real-time PCR was performed using the SYBR Green PCR Master Mix (TianGen Biotech, Beijing, China) and the PRISM 7500 real-time PCR detection system (ABI, USA). The following human primers (Generay Bioteach Co. Ltd, Shanghai, China) were used in this study: β-actin F, 5´-GAGACCTTCAACACCCCAGC-3´; β-actin R, 5´-ATGTCACGCACG

ATTTCCC-3′; MLH1 F, 5′-TTCTTACTCTTCATCAACCATCGTC-3′; MLH1 R, 5′-TTCTGGGGACTGATTTCTAAACTGA-3′; MSH2 F, 5′-GCCAAGAAGTTTCAAAGACAAGC-3′; MSH2 R, 5′-GGAGAAGTCAGAACGAAGATCAG-3′; MSH6 F, 5′-TAACGGTTCCTACCAATC-3′; MSH6 R, 5′-GGGATACAGCCTTTGACC-3′; PMS1 F, 5′-TTGTGCCCCTGGACTTTTCT-3′; PMS1 R, 5′-ATCTTCGGCTGCTTGATTTTCTC-3′; Nrf2 F, 5′-ACCTCCCTGTTGTTGACTT-3′; Nrf2 R, 5′-CACTTTATTCTTACCCCTCCT-3′; RFC4 F, 5′-TTCCAGGTGGTCCGTAAA-3′, RFC4 R, 5′-CAAGGATCGAGGAGTAGCT-3′.

**Western blotting analysis**

Protein lysate was extracted from cells using RIPA lysis buffer supplemented with 1 μM PMSF (Solarbio Science & Technology, Beijing, China) agitated at 4℃ for 30 min. The extracts were centrifuged at 12, 000 rpm for 15 min at 4˚C, and the supernatant was collected. A BCA protein assay kit (Pierce, Hercules, CA, USA) was used to determine the protein concentrations. Protein (40μg) were then loaded on 10% SDS–PAGE gel and the separated proteins transferred onto PVDF membranes. Membranes were routinely blocked in 5% nonfat milk in PBS for 2 h with agitation and washed. Then, the membrane was blotted with primary antibodies for 2 h. After washing, the membranes was incubated with secondary antibodies for 45 min at room temperature. All protein bands were visualized with the use of the enhanced chemiluminescence (7Sea Biotech).

**Hoechst 33342 staining assay**

THP-1 and Kasumi-1 cells were treated with 2μM of Ara-C for 24 h. Following treatment, the cells were collected, washed with PBS and fixed with 4% fixative solution for 30 min at room temperature. Subsequently, cells were washed again with

PBS and then incubated with Hoechst 33258 (10μg/mL) in dark at room temperature for 20 minutes. Finally, the cells were washed and re-suspended in PBS to observe nuclear morphological changes under a confocal microscope (Carl Zeiss, Oberkochen, Germany). Normal cell nuclei are homogeneously stained as blue, whereas the nuclei of apoptotic cells display chromatin condensation or nuclear fragmentation. Nuclei were counted from five different areas randomly for percentage of fragmented nuclei (apoptosis) in each group.

**Apoptosis assay**

Apoptosis was determined by double staining of annexinV-FITC and propidium iodide (PI) according to the manufacturer's instructions (7Sea Biotech, Shanghai, China). AML cells were harvested and washed with cold phosphate-buffered saline (PBS), then stained with 3.5 μL of AnnexinV-FITC and 5 μL of PI in dark. After that, the number of apoptotic cells were measured by flow cytometry using Cell Quest software (BD Biosciences, San Jose, CA, USA).

**ROS Detection**

The ROS levels induced by Ara-C in THP-1 and Kasumi-1 cells were detected using the probe 2′, 7′-dichlorodihydrofluorescein diacetate (DCFH-DA, Beyotime), which can be oxidized by intracellular oxygen to dichlorofluorescein, a highly fluorescent compound. After exposure to the indicated concentration of Ara-C (2μM), the cells were incubated with a final concentration of 10 μM DCFH-DA in the dark for 30 min at 37°C in a humidified atmosphere at 5% $CO_2$, after which the cells were washed three times with cold PBS to remove excess fluorescent probe. The cells were then resuspended in 300 μl of PBS and assessed for fluorescence intensity using a flow cytometer.

## Xenografted tumor model

NOD-SCID/IL2Rγc mice were purchased from Model Organisms Center (Shanghai, China). Stably transfected Nrf2 cells that were growing in the logarithmic phase were prepared. Cells were resuspended in PBS at a concentration of $5 \times 10^6$ cells/100 μL and then subcutaneously injected into the 5-week-old mice. For in vivo Ara-C treatment, twelve mices were dived into four groups. After the xenografts reached 0.5 cm in diameter, two of the groups were treated with Ara-C (60 mg/kg/day for 5 days) by intraperitoneal injection [35], the others were treated with PBS. Tumor growth was monitored by measurements of the length and width and the tumor volume was calculated using the equation $(L \times W^2)/2$. After mices were placed on the platform of BLT In-Vivo Imaging System (BLT Photon Tech., Guangzhou, China), fluorescence images were captured according to the manufacturer's instructions. Animals were euthanized, tumors were excised, weighed and paraffin-embedded. All experiments on mice were approved by the Institutional Animal Care and Use Committee of Guizhou Medical University, China.

## Immunocytochemical (ICC) and Immunohistochemical (IHC) staining

For ICC staining, the mononuclear cells of AML patients were fixed with 4% formaldehyde for 30 min. The mononuclear cells were washed with PBS for 3 times. Then cells was permeated into PBS with 0.1%Triton-X 100 at room temperature for 20 min. Sodium citrate antigen was repaired for 5 min and sealed with 5% bovine serum albumin for 1h at room temperature. Then incubated overnight at 4℃ with appropriate dilution (1:100 rabbit anti-Nrf2, 1:100 mouse anti-MSH2). The cells were washed with PBS for 3 times 10min. The cells were incubated with horseradish peroxide second antibody (1:200) for 1 h, and the cells were washed with PBS for 3 times.

Diaminobenzidine (Solarbio, Beijing, China) was incubated for 10 minutes, then washed with PBS for 10 minutes, and stained with hematoxylin for 1 minute. 50% 75% 95% concentration gradient ethanol dehydration, xylene transparency for 5 minutes, and finally the image was taken with a microscope. For IHC staining, the experiment was performed using manufacturer's instructions for kits SP-9001 (Zhong Shan-Golden Bridge Biological Technology). IHC assays were scored as previously describe [36].

### Bioinformatics analysis

The mRNA expression differences of the FLT3-ITD, NPM1 and KRAS gene between mutation AML and wild type in distinct types of cancer were determined using the Oncomine database (https://www.oncomine.org/). GeneMANIA (https://www.oncomine.org/) is a commonly used website for performing protein-protein interaction (PPI) network analysis and predicting the function of preferred genes. We predicted the function of the Nrf2, MSH2 and JUN gene and visualized the gene networks through GeneMANIA.

### Statistical analysis

GraphPad Prism 7.0 software (Graphpad Software, Inc, USA) was used to statistically analyze the data. Results were presented as mean ± standard deviation (SD). Statistical significance was determined based on a Student's t-test or one-way ANOVA. A P value of less than 0.05 was considered statistically significant.

## Results

### 1. Higher tumor mutation burden in AML patients with Nrf2 overexpression

With the development of the whole-genome sequencing technology, the increase of tumor gene mutation burden has been found to be one of the important reasons for relapsed and drug resistance in AML [37]. First of all, AML patient specimens were divided into two groups either expressing high or low levels of Nrf2 based on qRT-PCR, using the median Nrf2 expression levels as cut-off values. Then, we used whole-exon sequencing to detect gene mutations and calculated the tumor mutation burden values based on the mutation site. The tumor mutation burden values in the Nrf2-High expression group was significantly higher than that in the Nrf2-Low group (11.21 ±0.459 mut/Mb vs. 8.82 ±0.670 mut/Mb ($P < 0.05$)) (Fig.1a). And disease-related gene mutations were shown in Fig. 1c. In addition, patients in the Nrf2-High group had more remaining blast cells and less remission after standard chemotherapy, which had a higher risk of relapsed or drug resistance (Fig.1b). To investigate the role of Nrf2 in AML patients with gene mutations, we examined the gene expression level of Nrf2 in different types of gene mutations using the Oncomine database. We noticed that the expression of Nrf2 was upregulated in AML patients with FLT3-ITD, NPM1, KRAS positive mutations (Fig. 1d). We further analyzed Nrf2 protein expression level in 7 non-mutation and 7 mutation AML patients by western blotting. The results showed that the protein level of Nrf2 in mutation group was higher than that in non-mutation group ($P < 0.01$, Fig. 1e, f). Then we compared the mRNA levels of Nrf2 in mutated and non-mutated AML samples. The results showed that the Nrf2 expression in tumor cells of mutated group was significantly higher than that in non-mutated group ($P < 0.05$, Fig. 1g). Therefore, we preliminarily concluded that the high expression of Nrf2 in AML was related to the high tumor mutation burden.

**2. High expression of Nrf2 inhibited DNA mismatch repair pathway in AML**

In order to further understand the molecular mechanism of Nrf2 on tumor mutation burden rate in AML, we examined RNAseq in the above patients, removed the unqualified samples, and analyzed the difference of gene expression. As shown in Fig. 2a, the heat map illustrated the differentially expressed genes between Nrf2-High and Nrf2-Low group (Fig. 2a). We then performed KEGG pathway enrichment analysis on the genes differentially expressed in AML samples. The results indicated that DNA mismatch repair pathway was significantly inhibited in AML with high expression of Nrf2 (Fig. 2b). It is well-known that MMR pathway is an important way to influence point mutation [38]. Thus, qRT-PCR analysis was employed to identify MMR genes. We found that mRNA expression of MSH2 in Nrf2-Low group was significantly higher than that of Nrf2-High group ($P < 0.05$, Fig. 2c). A similar tendency was observed in protein level of MSH2 by western blotting. MSH2 were also decreased in Nrf2-High expressing AML patients ($P < 0.05$, Fig. 2d, e). Finally, we performed ICC detection in AML patients with different Nrf2 expression. The ICC staining results showed that patients in high Nrf2 expression group had lower level of MSH2 when compared with patients in Nrf2-Low group (Fig. 2f). These results suggested that high Nrf2 expression inhibited MSH2 in AML.

**3. High Nrf2 expression increased the resistance of AML cell lines to Ara-C while inhibited the expression of MSH2.**

According to the above results in clinical samples, we speculated that Nrf2 high expression inhibited the expression of MSH2, caused MMR deficiency and increased the tumor mutation burden, which can induce gene instability-dependent drug resistance. To test this hypothesis, we overexpressed and silenced Nrf2 in two different AML cell lines (THP-1 and Kasumi-1). The Nrf2 expression levels in these cell lines

were verified by Western blotting and qRT-PCR (Fig. 3a, b and c). Then, hoechst-33258 stain was applied to evaluate the effect of Nrf2 on nuclear fragmentation (apoptosis marker) in THP-1 and Kasumi-1 cells. The data showed that Nrf2 overexpression in AML cell lines decreased the apoptosis of cells treated with 2μM Ara-C for 24 h (Fig. 3d, e). Besides, we confirmed that Ara-C led to the accumulation of MSH2 protein in a concentration-dependent manner (Figure S1A, B). Moreover, we found that Nrf2 overexpression potently decreased the protein level of MSH2, whereas MSH2 protein levels were increased upon Nrf2 downregulation in THP-1 and Kasumi-1 cells (Fig. 3f-i). Therefore, Nrf2 was shown to promote Ara-C resistance in AML cells by inhibiting MSH2.

**4. AML cells with Nrf2 high expression had a higher risk of mutant drug resistance in vivo**

To confirm the effect of Nrf2 in AML cell growth in vivo, the NOD-SCID/IL2Rγc mice xenograft model was established by subcutaneous injection of Nrf2 or empty vector transfected THP-1 cells. And the mice were treated with Ara-C as soon as the tumor became palpable. As shown in Fig.4a-b, Nrf2 overexpression resulted in a significant increase in tumor growth compared with that in the EV group. Nrf2 overexpression effectively promoted the tumor volumes (Fig. 4c) and tumor weights (Fig.4d) compared to the EV group ($P$<0.05). Moreover, treatment with Ara-C resulted in a significant reduction in tumor growth. As shown in Fig. 4e, mice transplanted with L-Nrf2 cells had the shortest survival, whereas mice transplanted with EV cells had a prolonged overall survival ($P$<0.05). Furthermore, MSH2 expression was examined in paraffin-embedded tumor tissues by an IHC assay. In vivo, there was no significant alterations in MSH2 between the Nrf2 overexpression group and the EV group without Ara-C

310 treatment (Fig. 4f). However, after treatment with Ara-C, MSH2 expression was still
311 weaken in the Nrf2 overexpression group, but increased in the EV group (Fig. 4g).
312 Therefore, these data demonstrated that Nrf2 overexpression promoted tumor growth
313 and inhibited MSH2, which contributed to a higher risk of mutant drug resistance in
314 vivo.

315 **5. The high expression of Nrf2 inhibited MSH2 in a ROS-independent manner.**

316 When tumor cells were stimulated by chemotherapy, Nrf2, as an important transcription
317 factor of antioxidant stress, could significantly inhibit the production of ROS [39]. ROS
318 is also an important factor that initiates the cellular MMR system [40]. Previous
319 research had shown that Nrf2 regulated apoptosis of AML cell lines. Next, the
320 mechanism of whether Nrf2 induced DNA MMR regulated ROS was investigated. We
321 observed ROS levels in these cell lines at 24 h after Ara-C treatment. The results
322 showed that ROS was higher than that before 2μM Ara-C treatment of cells in each
323 group. However, the increased ROS in the Nrf2 overexpressing group was significantly
324 lower than that of the EV group and the control group ($P < 0.05$, Fig. 5a). The apoptotic
325 rate was measured by Annexin V/PI assay after treating Nrf2-overexpressing cells with
326 2μM Ara-C for 24 h. The apoptosis of Nrf2 overexpressing group was significantly
327 decreased in comparison with EV and control group ($P < 0.05$, Fig. 5b).

328 If Ara-C induced ROS production can account for the increase of MSH2 protein in
329 AML cells, $H_2O_2$ should increase intracellular ROS and elevate MSH2 expression in
330 Nrf2 overexpressing cells. To examine whether there was an intrinsic link between ROS
331 accumulation and the protein levels of MSH2 in AML cells, we pretreated THP-1 and
332 Kasumi-1 cells with $H_2O_2$ (50 μM) for 6 h in Nrf2 overexpressing cells. The results
333 showed that MSH2 expression in the Nrf2 overexpression group pretreated with $H_2O_2$

was still weakened (Fig. 5c, d). In addition, we pretreated the Nrf2 down-regulation group with ROS scavenger NAC (5 mM) for 2 h and then exposure to Ara-C for 24 h. Western blot assays showed that THP-1 and Kasumi-1 cells treated with Ara-C in combination with NAC weaken MSH2 expression upon Nrf2 knockdown, and there was no significant difference compared with EV group (Fig. 5e, f). Collectively, these findings revealed that Nrf2 inhibited ROS elevtion induced by Ara-C, leading to resistance of AML cells to chemotherapy. However, the ROS level of the Nrf2-expressing cells had no significant effect on the MSH2 expression.

**6. Nrf2 inhibited MSH2 expression in AML cells by activating the JNK/c-Jun signaling pathway**

Based on the above results, we found that the inhibition of MSH2 by Nrf2 was not depended on the ROS accumulation. To investigate the underlying mechanism, we used GeneMANIA's PPI network to reveal the relationship between Nrf2 and MSH2. The results showed that Nrf2 might regulate MSH2 through the JUN signal pathway (Fig. 6a). We quantified the expressions of c-Jun and c-Jun N-terminal kinase (JNK) by western blotting with the Nrf2 overexpression. The results showed that Nrf2 was positively correlated with c-Jun. Nrf2 overexpression in THP-1 and Kasumi-1 cells dramatically increased phosphorylated JNK and c-Jun levels compared to EV cells (Fig. 6b-e). Furthermore, we selected a JNK inhibitor (SP600125) to complete the following experiment. Then, AML cells were treated with 10μM SP600125 for 24h. Although the expression of Nrf2 in THP-1 and Kasumi-1 cells changed slightly, the protein levels of pJNK and p-c-Jun were decreased. Conversely, the protein levels of MSH2 were increased in Nrf2 overexpressing cells (Fig. 6b-e). In summary, these data indicated

that Nrf2 overexpression inhibited MSH2 expression through activating JNK/c-Jun signaling pathway.

## Discussion

Chemoresistance is one of the major difficulties during cancer chemotherapy. According to whether the occurrence of drug resistance is related to gene mutation, it can be divided into gene instability-dependent and independent drug resistance. Previous reports in AML, and other solid tumors have shown that Nrf2 is associated with resistance to chemotherapeutic agents [41-43]. The high Nrf2 expression can lead to the gene instability-independent drug resistance in AML, and its mechanism is mostly related to the activation of NF-kB [44]. However, there are few reports about the relationship between Nrf2 and gene instability-dependent drug resistance. In the current study, we characterized the role of Nrf2 in AML gene instability-dependent chemotherapy resistance and investigated its underlying molecular basis. We found that Nrf2 overexpression protected the AML cells from apoptosis induced by Ara-C in vitro and increased the risk of gene mutant drug resistance in vivo by suppressing MSH2 protein expression.

According to the whole-exon sequencing analysis, AML patients with high Nrf2 expression had higher tumor mutation burden. Furthermore, patients in the Nrf2-High group had more remaining blast cells and less remission after standard chemotherapy, implicating Nrf2 expression was associated with relapse and chemotherapy-resistance. In addition, compared the differences of genes and pathways between the Nrf2 high/low groups of AML patients by RNAseq, we found that high Nrf2 expression significantly inhibited the DNA MMR pathway leading to genomic instability in AML patients. MMR plays crucial role in regulating tumor gene mutation[45]. The abnormal

expression of MMR related proteins is also related to tumor drug resistance [46]. In the case of leukemia, Diouf et al. observed that the protein level of DNA mismatch repair protein MSH2 in 11% of childhood acute lymphoblastic leukemia cells decreased significantly and was resistant to mercaptopurine [47]. According to the research by Mao et al., 34.0% of AML patients had MMR gene mutation or MLH1 promoter methylation, and the incidence of MMR deficiency in refractory or recurrent AML patients was significantly higher than that in newly diagnosed patients [48]. These findings indicate that DNA MMR is much crucial in progression of leukemia. In our study, Nrf2 expression mainly induced gene instability-dependent drug resistance in AML by inhibiting DNA MMR, which was consistent with the above findings.

High Nrf2 expression caused MMR deficiency and increased the tumor mutation burden, whereas its exact roles in AML remain understudied. Here, we provided the significant evidence that Nrf2 overexpression could induce drug resistance in AML by suppressing MSH2. In vitro, Nrf2 overexpression protected the AML cells from apoptosis induced by Ara-C. Notably, MSH2 was suppressed by the upregulation of Nrf2, while MSH2 protein levels were increased upon Nrf2 downregulation in THP-1 and Kasumi-1 cells. In addition, we found that mice bearing AML cells with Nrf2 overexpression demonstrated higher leukemia infiltration, lower survival and MMR deficiency in vivo. In sum, these results implied that Nrf2 overexpression lead to gene instability-dependent drug resistance through suppressing MSH2 expression.

Understanding the functional mechanism of Nrf2 suppressed DNA MMR in AML will greatly facilitate development of drug resistance therapy. The continuous activation of Nrf2 leads to the relative decrease of intracellular ROS. A certain concentration of ROS can promote cell growth [49]. And excessive accumulation of ROS can increase the

methylation level of MMR-related factors MLH1 and MSH2 promoter, resulting in decreased expression and loss of function [40]. As the upstream regulatory genes of MSH2, mTOR, HERC1, PRKCZ and PIK3C2B, are mutated, it will lead to a decrease in MSH2 expression and a MMR deficiency state in tumor cells [47]. In this study, after the cells treatment with Ara-C, a significant increase in ROS generation was detected by flow cytometry and DCFH-DA in the Nrf2 overexpressing group, while the increasing levels of ROS in Nrf2 overexpressing group was significantly lower than that in empty vector group and control group. To further investigate the effect of intracellular ROS on MSH2 protein expression, we changed ROS levels in THP-1 and Kasumi-1 cells. When NAC, a ROS scavenger, was applied, there was no significant difference in MSH2 expression in Nrf2 silent group compared with EV group. However, Nrf2 overexpression still suppressed MSH2 expression after Nrf2 overexpressing cells treatment with Ara-C in combination with $H_2O_2$. This finding demonstrates that regulation of MSH2 by Nrf2 is not depended on ROS signal.

Our research team had previously proved that overexpression of heme oxygenase-1 (one of Nrf2 target genes) promoted proliferation and increased resistance to Ara-C induced apoptosis of AML cells in vitro and the leukemia's progression of AML in vivo by activating the JNK/c-Jun signaling pathway [50]. The c-Jun oncogene is a member of the activator protein-1 (AP-1) family of transcription factors that is phosphorylated and activated by the JNK [51]. Previous study suggested that shRNA-mediated inhibition of Jun decreased AML cell survival and propagation in vivo [52]. These studies demonstrated that JNK/c-Jun activation played an important role in AML. Given the significance of JNK/c-Jun signaling pathway in AML, our research provided novel insights that Nrf2 inhibited MSH2 expression and promoted AML gene instability-dependent chemoresistance by activating JNK/c-Jun signaling pathway (Fig.

7). The phosphorylation levels of JNK and c-Jun proteins were noted to be dramatically increased in Nrf2 overespressing cells compared to control cells. JNK/c-Jun could suppressed MSH2 protein expression in Nrf2 overexpressing cells. In summary, Nrf2 overexpression enhanced chemoresistance and decreased the MSH2 expression by activing JNK/c-Jun signal in AML cells.

However, the mechanism underlying activation of Nrf2 on JNK remains unclear. Notably, upon UV irradiation, a cooperation of p53 and the c-Jun pathway activates transcription of mismatch repair gene MSH2 [53]. According to references and our results, the high level of Nrf2 exerts an MMR deficiency effects on tumor cells by JNK/c-Jun signaling pathway which probably suppresses P53 or up-regulates DUSP1 [54, 55], but this postulation still needs further exploration.

## Conclusions

In conclusion, our results provide evidence that high Nrf2 expression inhibites MSH2 expression through activating JNK/c-Jun signaling pathway, playing a key role in frequency of gene mutation in tumor cells, thus achieving drug resistance in AML. We propose an underlying regulatory mechanism that Nrf2 induces gene mutation-dependent drug resistance of AML.

## Abbreviations

AML: Chromatin immunoprecipitation; Nrf2: Nuclear factor erythroid 2-related factor 2; MMR: mismatch repair; MSI: microsatellite instability; ROS: reactive oxygen species; Ara-C: cytarabine; RNAseq: transcriptome sequencing; KEGG: Kypto encyclopedia of genes and genomes; ICC: Immunocytochemistry IHC:

Immunochemistry; WB: Western blot .NAC: N-acetylcysteine; JNK: c-Jun N-terminal kinase.

## Acknowledgments

The authors sincerely thank Haiyang Hao for his support and suggestions for this study.

## Authors' contributions

Study design and data collection: PL, MD and JW; PW performed the clinical analysis; PL mainly performed the experiments; Data analysis: PL, CP and QF; Manuscript preparation: PL. All authors read and approved the final manuscript.

## Funding

This work was supported by the National Natural Science Foundation of China (No. 81760670 and 81960032), Translational Research Grant of NCRCH (2020ZKPB03).

## Availability of data and materials

All data in our study are available upon request.

## Ethics approval and consent to participate

This study was approved by the ethics committee of Affiliated Hospital of Guizhou Medical University and Guizhou Medical University, and written informed consents were obtained before any operation to patients. The authors confirmed that we have obtained written consent from the patients to publish this manuscript.

## Consent for publication

Not applicable.

## Competing interests

The authors declare no conflicts of interest.

## References


1. Döhner, H., D.J. Weisdorf, and C.D. Bloomfield, Acute myeloid leukemia. New England Journal of Medicine. 2015; 373: 1136-1152.
2. Döhner, H., E. Estey, D. Grimwade, S. Amadori, F.R. Appelbaum, T. Büchner, et al. Diagnosis and management of AML in adults: 2017 ELN recommendations from an international expert panel. Blood. 2017; 129: 424-447.
3. Mims, A.S. and W. Blum. Progress in the problem of relapsed or refractory acute myeloid leukemia. Current Opinion in Hematology. 2019; 26: 88-95.
4. Jang, J.E., J.I. Eom, H.K. Jeung, H. Chung, Y. R. Kim, J.S. Kim, et al. PERK/NRF2 and autophagy form a resistance mechanism against G9a inhibition in leukemia stem cells. Journal of Experimental & Clinical Cancer Research. 2020; 39(1): 66.
5. Lv, Y., G. Shao, Q. Zhang, X. Wang, Y. Meng, L. Wang, F., et al. The antimicrobial peptide PFR induces necroptosis mediated by ER stress and elevated cytoplasmic calcium and mitochondrial ROS levels: cooperation with Ara-C to act against acute myeloid leukemia. Signal transduction and targeted therapy. 2019; 4: 38.
6. Dumontet, C. and M. Jordan. Microtubule-binding agents: a dynamic field of cancer therapeutics. Nature reviews. Drug discovery. 2010; 9: 790-803.
7. Steinhart, L., K. Belz, and S. Fulda. Smac mimetic and demethylating agents synergistically trigger cell death in acute myeloid leukemia cells and overcome apoptosis resistance by inducing necroptosis. Cell death & disease. 2013; 4: e802.
8. Long, J., W. Fang, L. Chang, W. Gao, Y. Shen, M. Jia, et al. Targeting HDAC3, a new partner protein of AKT in the reversal of chemoresistance in acute myeloid leukemia via DNA damage response. Leukemia. 2017; 31: 2761-2770.

9. Caiado, F., D. Maia-Silva, C. Jardim, N. Schmolka, T. Carvalho, C. Reforço, et al. Lineage tracing of acute myeloid leukemia reveals the impact of hypomethylating agents on chemoresistance selection. Nature communications. 2019; 10: 4986.
10. Xia, B., C. Tian, S. Guo, L. Zhang, D. Zhao, F. Qu, et al. c-Myc plays part in drug resistance mediated by bone marrow stromal cells in acute myeloid leukemia. Leukemia research. 2015; 39: 92-99.
11. Dumas, P., C. Naudin, S. Martin-Lannerée, B. Izac, L. Casetti, O. Mansier, et al. viaHematopoietic niche drives FLT3-ITD acute myeloid leukemia resistance to quizartinib STAT5-and hypoxia-dependent upregulation of AXL. Haematologica. 2019; 104: 2017-2027.
12. Panieri, E., A. Buha, P. Telkoparan-Akillilar, D. Cevik, D. Kouretas, A. Veskoukis, et al. Potential Applications of NRF2 Modulators in Cancer Therapy. Antioxidants (Basel). 2020; 9, 193.
13. Rushworth, S. and D. Macewan. The role of nrf2 and cytoprotection in regulating chemotherapy resistance of human leukemia cells. Cancers. 2011; 3: 1605-1621.
14. Niture, S. and A. Jaiswal. Nrf2-induced antiapoptotic Bcl-xL protein enhances cell survival and drug resistance. Free radical biology & medicine. 2013; 57: 119-131.
15. Panieri, E. and L. Saso. Potential Applications of NRF2 Inhibitors in Cancer Therapy. Oxidative medicine and cellular longevity. 2019; 2019: 8592348.
16. Roh, J., H. Jang, E. Kim, and D. Shin. Targeting of the Glutathione, Thioredoxin, and Nrf2 Antioxidant Systems in Head and Neck Cancer. Antioxidants & redox signaling. 2017; 27: 106-114.
17. Jeddi, F., N. Soozangar, M. Sadeghi, M. Somi, M. Shirmohamadi, A. Eftekhar-Sadat, et al. Nrf2 overexpression is associated with P-glycoprotein upregulation in gastric cancer. Biomedicine & pharmacotherapy. 2018; 97: 286-292.
18. Ma, C., Q. Lv, K. Zhang, Y. Tang, Y. Zhang, Y. Shen, et al. NRF2-GPX4/SOD2 axis imparts resistance to EGFR-tyrosine kinase inhibitors in non-small-cell lung cancer cells. Acta pharmacologica Sinica. 2020.
19. Ma, S., C. Paiboonrungruan, T. Yan, K. Williams, M. Major, and X. Chen. Targeted therapy of esophageal squamous cell carcinoma: the NRF2 signaling

pathway as target. Annals of the New York Academy of Sciences. 2018; 1434: 164-172.

20. Almeida, M., M. Soares, A. Ramalhinho, J. Moutinho, L. Breitenfeld, and L. Pereira. The prognostic value of NRF2 in breast cancer patients: a systematic review with meta-analysis. Breast cancer research and treatment. 2020; 179: 523-532.

21. Zhang L, N. Wang, S. Zhou, W. Ye, G. Jing, M. Zhang. Propofol induces proliferation and invasion of gallbladder cancer cells through activation of Nrf2. Journal of Experimental & Clinical Cancer Research. 2012; 31(1): 66.

22. Bao, L., J. Wu, M. Dodson, E. Rojo de la Vega, Y. Ning, Z. Zhang, et al. ABCF2, an Nrf2 target gene, contributes to cisplatin resistance in ovarian cancer cells. Molecular carcinogenesis. 2017; 56: 1543-1553.

23. Wang, X., J. Hayes, and C. Wolf. Generation of a stable antioxidant response element-driven reporter gene cell line and its use to show redox-dependent activation of nrf2 by cancer chemotherapeutic agents. Cancer research. 2006; 66: 10983-10994.

24. Méndez-García, L., M. Martínez-Castillo, N. Villegas-Sepúlveda, L. Orozco, and E. Córdova. Curcumin induces p53-independent inactivation of Nrf2 during oxidative stress-induced apoptosis. Human & experimental toxicology. 2019; 38: 951-961.

25. Tung, M., P. Lin, Y. Wang, T. He, M. Lee, S. Yeh, et al. Mutant p53 confers chemoresistance in non-small cell lung cancer by upregulating Nrf2. Oncotarget. 2015; 6: 41692-41705.

26. Sengupta, A., S. Mukherjee, S. Ghosh, T. Keswani, S. Sarkar, G. Majumdar, et al. Partial impairment of late-stage autophagic flux in murine splenocytes leads to sqstm1/p62 mediated nrf2-keap1 antioxidant pathway activation and induced proteasome-mediated degradation in malaria. Microbial pathogenesis, 2020: 104289.

27. Niture, S. and A. Jaiswal. Nrf2 protein up-regulates antiapoptotic protein Bcl-2 and prevents cellular apoptosis. The Journal of biological chemistry. 2012; 287: 9873-9886.

28. Lord, C.J. and A. Ashworth. The DNA damage response and cancer therapy. Nature. 2012; 481: 287-294.

29. Karran, P., J. Offman, and M. Bignami. Human mismatch repair, drug-induced DNA damage, and secondary cancer. Biochimie. 2003; 85: 1149-1160.
30. Xavier, A., M. Olsen, L. Lavik, J. Johansen, A. Singh, W. Sjursen, et al. Comprehensive mismatch repair gene panel identifies variants in patients with Lynch-like syndrome. Molecular genetics & genomic medicine. 2019; 7: e850.
31. Akbari, M., S. Zhang, D. Cragun, J. Lee, D. Coppola, J. McLaughlin, et al. Correlation between germline mutations in MMR genes and microsatellite instability in ovarian cancer specimens. Familial cancer. 2017; 16: 351-355.
32. McCarthy, A., J. Capo-Chichi, T. Spence, S. Grenier, T. Stockley, S. Kamel-Reid, et al. Heterogenous loss of mismatch repair (MMR) protein expression: a challenge for immunohistochemical interpretation and microsatellite instability (MSI) evaluation. The journal of pathology Clinical research. 2019; 5: 115-129.
33. Humbert, O., T. Hermine, H. Hernandez, T. Bouget, J. Selves, G. Laurent, et al. Implication of protein kinase C in the regulation of DNA mismatch repair protein expression and function. The Journal of biological chemistry. 2002; 277: 18061-18068.
34. Pearsall, E., L. Lincz, and K. Skelding. The Role of DNA Repair Pathways in AML Chemosensitivity. Current drug targets. 2018; 19: 1205-1219.
35. Schimmer, A. Novel Mitochondrial Mechanisms of Cytarabine Resistance in Primary AML Cells. Cancer discovery. 2017; 7: 670-672.
36. Guo, C. M., C. Gao, D. T. Zhao, J.H. Li, J.X. Wang, X.J. Sun, et al. A novel ETV6-miR-429-CRKL regulatory circuitry contributes to aggressiveness of hepatocellular carcinoma. Journal of Experimental & Clinical Cancer Research. 2020; 39: 70.
37. Li, D., T. J. Ley, D. E. Larson, C. A. Miller, D. C. Koboldt, J. S. Welch, et al. Clonal evolution in relapsed acute myeloid leukaemia revealed by whole-genome sequencing. Nature. 2012; 481: 506-510.
38. Hechtman, J., S. Rana, S. Middha, Z. Stadler, A. Latham, R. Benayed, et al. Retained mismatch repair protein expression occurs in approximately 6% of microsatellite instability-high cancers and is associated with missense mutations in mismatch repair genes. Modern pathology. 2020; 33: 871-879.
39. Hyun, D. Insights into the New Cancer Therapy through Redox Homeostasis and Metabolic Shifts. Cancers. 2020; 12: 1822.

602 40. Gunes, S., A. Agarwal, R. Henkel, A. Mahmutoglu, R. Sharma, S. Esteves, et
603 al. Association between promoter methylation of MLH1 and MSH2 and
604 reactive oxygen species in oligozoospermic men-A pilot study. Andrologia.
605 2018; 50: e12903.
606 41. Karathedath, S., B. Rajamani, S. Musheer Aalam, A. Abraham, S. Varatharajan,
607 P. Krishnamurthy, et al. Role of NF-E2 related factor 2 (Nrf2) on chemotherapy
608 resistance in acute myeloid leukemia (AML) and the effect of pharmacological
609 inhibition of Nrf2. PloS one. 2017; 12: e0177227.
610 42. Sun, X., S. Wang, J. Gai, J. Guan, and Q. Li. SIRT5 Promotes Cisplatin
611 Resistance in Ovarian Cancer by Suppressing DNA Damage in a ROS-
612 Dependent Manner via Regulation of the Nrf2/HO-1 Pathway. Frontiers in
613 Oncology. 2019; 9: 754.
614 43. Zhou, Y., Y. Zhou, M. Yang, K. Wang, Y. Liu, M. Zhang, et al. Digoxin
615 sensitizes gemcitabine-resistant pancreatic cancer cells to gemcitabine via
616 inhibiting Nrf2 signaling pathway. Redox Biology. 2019; 22: 101131.
617 44. Rushworth, S., L. Zaitseva, M. Murray, N. Shah, K. Bowles, and D. MacEwan.
618 The high Nrf2 expression in human acute myeloid leukemia is driven by NF-
619 κB and underlies its chemo-resistance. Blood. 2012; 120: 5188-5198.
620 45. Wang, W., Y. Lee, and Y. Lai. PMS2 gene mutation results in DNA mismatch
621 repair system failure in a case of adult granulosa cell tumor. Journal of ovarian
622 research. 2017; 10: 22.
623 46. Pećina-Šlaus, N., A. Kafka, I. Salamon, and A. Bukovac. Mismatch Repair
624 Pathway, Genome Stability and Cancer. Frontiers in molecular biosciences.
625 2020; 7: 122.
626 47. Diouf, B., Q. Cheng, N. Krynetskaia, W. Yang, M. Cheok, et al. Somatic
627 deletions of genes regulating MSH2 protein stability cause DNA mismatch
628 repair deficiency and drug resistance in human leukemia cells. Nature medicine.
629 2011; 17: 1298-1303.
630 48. Mao, G., F. Yuan, K. Absher, C. Jennings, D. Howard, C. Jordan, et al.
631 Preferential loss of mismatch repair function in refractory and relapsed acute
632 myeloid leukemia: potential contribution to AML progression. Cell research.
633 2008; 18: 281-289.

49. Warfel, N., A. Sainz, J. Song, and A. Kraft. PIM Kinase Inhibitors Kill Hypoxic Tumor Cells by Reducing Nrf2 Signaling and Increasing Reactive Oxygen Species. Molecular cancer therapeutics. 2016; 15: 1637-1647.
50. Lin, X., Q. Fang, S. Chen, N. Zhe, Q. Chai, M. Yu, et al. Heme oxygenase-1 suppresses the apoptosis of acute myeloid leukemia cells via the JNK/c-JUN signaling pathway. Leukemia research. 2015; 39 (5): 544-552.
51. Koshizuka, T. and N. Inoue. Activation of c-Jun by human cytomegalovirus UL42 through JNK activation. PloS one. 2020; 15: e0232635.
52. Zhou, Martinez, Di, Marcantonio, and Solanki-Patel. JUN is a key transcriptional regulator of the unfolded protein response in acute myeloid leukemia. Leukemia. 2017, 31: 1196-1205.
53. Scherer, S., S. Maier, M. Seifert, R. Hanselmann, K. Zang, H. Muller-Hermelink, et al. p53 and c-Jun functionally synergize in the regulation of the DNA repair gene hMSH2 in response to UV. The Journal of biological chemistry. 2000; 275: 37469-37473.
54. Taylor, C., Q. Zheng, Z. Liu, and J. Thompson. Role of p38 and JNK MAPK signaling pathways and tumor suppressor p53 on induction of apoptosis in response to Ad-eIF5A1 in A549 lung cancer cells. Molecular cancer. 2013; 12: 35.
55. Lin, P., Y. Ren, X. Yan, Y.W. Luo, Zhang H., M. Kesarwani, et al. The high NRF2 expression confers chemotherapy resistance partly through up-regulated DUSP1 in myelodysplastic syndromes. Haematologica. 2019; 104(3): 485-496.

# Table

Table1 Characteristics of patient samples

| Patients no. | Age (years) | Gender | FAB subtype | Cell count($\times 10^9$/l) | | | BM Blast (%) | Karyotype |
|---|---|---|---|---|---|---|---|---|
| | | | | WBC | HB | PLT | | |
| 1 | 45 | M | M2 | 30.1 | 87 | 9 | 70.5 | 46,XX,t(8,21)(q22;q22) |
| 2 | 41 | F | M5 | 14.58 | 103 | 62 | 60.4 | 46,XX |
| 3 | 49 | M | M4 | 4.84 | 69 | 100 | 88 | 45,XY,-7 |
| 4 | 65 | M | M5 | 220 | 85 | 52 | 86.8 | 46,XY |
| 5 | 61 | F | M5 | 4.61 | 71 | 197 | 32.4 | 46,XX |
| 6 | 48 | F | M5 | 17.8 | 57 | 41 | 33.9 | 46,XX |
| 7 | 51 | F | M5 | 21.17 | 109 | 231 | 90 | 46,XX |
| 8 | 54 | M | M2 | 143.19 | 60 | 15 | 92.3 | 47,XY,+8 |
| 9 | 29 | F | M2 | 197.12 | 65 | 23 | 71 | 46,XX |
| 10 | 21 | M | M2 | 269.13 | 42 | 53 | 26.4 | 46,XY |
| 11 | 35 | M | M2 | 31.65 | 90 | 330 | 31 | 46,XY |
| 12 | 55 | M | M5 | 88.30 | 59 | 17 | 69 | 46,XY |
| 13 | 20 | M | M2 | 6.1 | 68 | 12 | 68 | 46,XY |
| 14 | 43 | F | M5 | 0.36 | 46 | 15 | 35.5 | 46,XX |
| 15 | 62 | M | M2 | 40.49 | 99 | 19 | 65.7 | 46,XY |
| 16 | 79 | M | M2 | 110.18 | 30 | 8 | 49.4 | 46,XY |
| 17 | 29 | F | M2 | 41.42 | 79 | 10 | 68.4 | 46,XX |
| 18 | 30 | F | M2 | 8.81 | 106 | 20 | 59.5 | 46,XX |
| 19 | 49 | M | M5 | 107.14 | 29 | 14 | 47.3 | 46,XY |
| 20 | 44 | M | M2 | 179.46 | 79 | 64 | 92.4 | 46,XY |
| 21 | 32 | F | M5 | 31.43 | 75 | 94 | 72.1 | 46,XX |
| 22 | 48 | F | M2 | 334.80 | 52 | 501 | 60.1 | 46,XX,t(6;9)(p23;q34) |
| 23 | 74 | M | M2 | 70.08 | 50 | 30 | 73.3 | 46,XY |
| 24 | 40 | F | M5 | 15.4 | 63 | 21 | 33.8 | 46,XX |
| 25 | 55 | M | M4 | 42.84 | 52 | 56 | 48.6 | 46,XY |
| 26 | 20 | F | M2 | 8.7 | 125 | 159 | 34.4 | 46,XX |
| 27 | 49 | M | M5 | 0.35 | 64 | 16 | 49.4 | 46,XY |
| 28 | 22 | F | M2 | 142.44 | 40 | 29 | 82.7 | 46,XX |
| 29 | 64 | F | M2 | 4.37 | 52 | 27 | 33 | 46,XX |
| 30 | 64 | F | M5 | 2.5 | 72 | 36 | 55.8 | 46,XX |
| 31 | 21 | M | M5 | 4.01 | 62 | 30 | 47.2 | 46,XY |
| 32 | 53 | M | M4 | 30.95 | 95 | 15 | 74.8 | 46,XY,t(3;5)(p25;q22) |
| 33 | 74 | M | M2 | 12.86 | 65 | 310 | 51.5 | 46,XY |

Abbreviations: BM, bone marrow; F, female; FAB, French–American–British; HB, hemoglobin; M, male; PLT, platelet; WBC, white blood cell.

# Figures

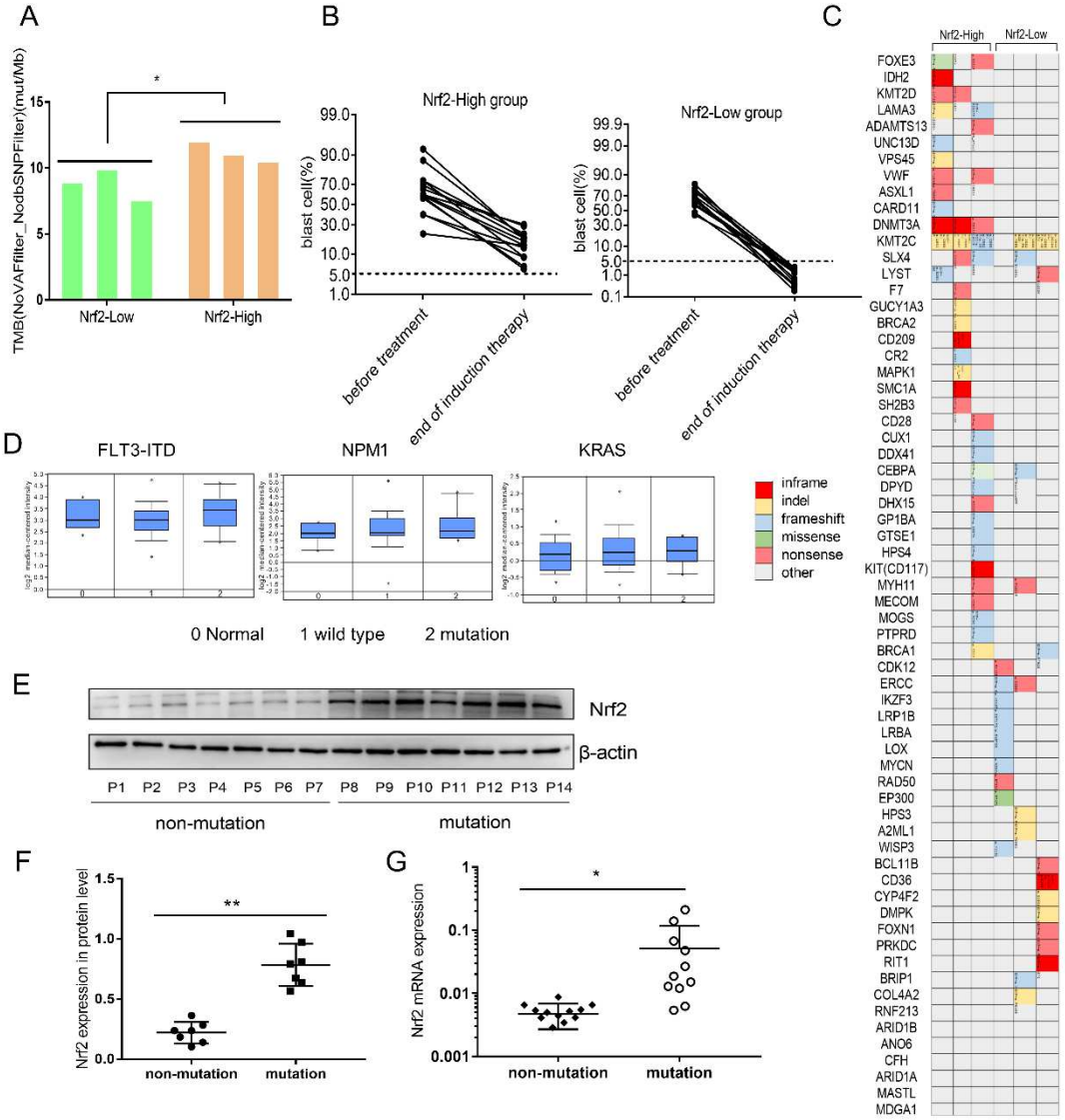


**Fig. 1** Nrf2 expression and tumor mutation burden in AML. **a** TMB values of mutation sites in Nrf2 high/low expression group. **b** The percentage of blast cells were detected in 15 matched Nrf2 high/low AML specimens. **c** Disease-related gene mutations were shown in AML patients with high/low expression of Nrf2 by whole-exon sequencing. **d** Studies in the Oncomine database showed higher mRNA expression of Nrf2 in AML patients with FLT3-ITD, NPM1, KRAS positive mutations. **e** Expression levels of Nrf2 protein were detected in 14 AML specimens by western blotting (P: patient). **f** Quantification of Nrf2 expression in AML samples. **g** mRNA expression of Nrf2 in AML by qRT-PCR. Results are presented as means ± SD; TMB, tumor mutation burden. *p < 0.05, **p < 0.01.

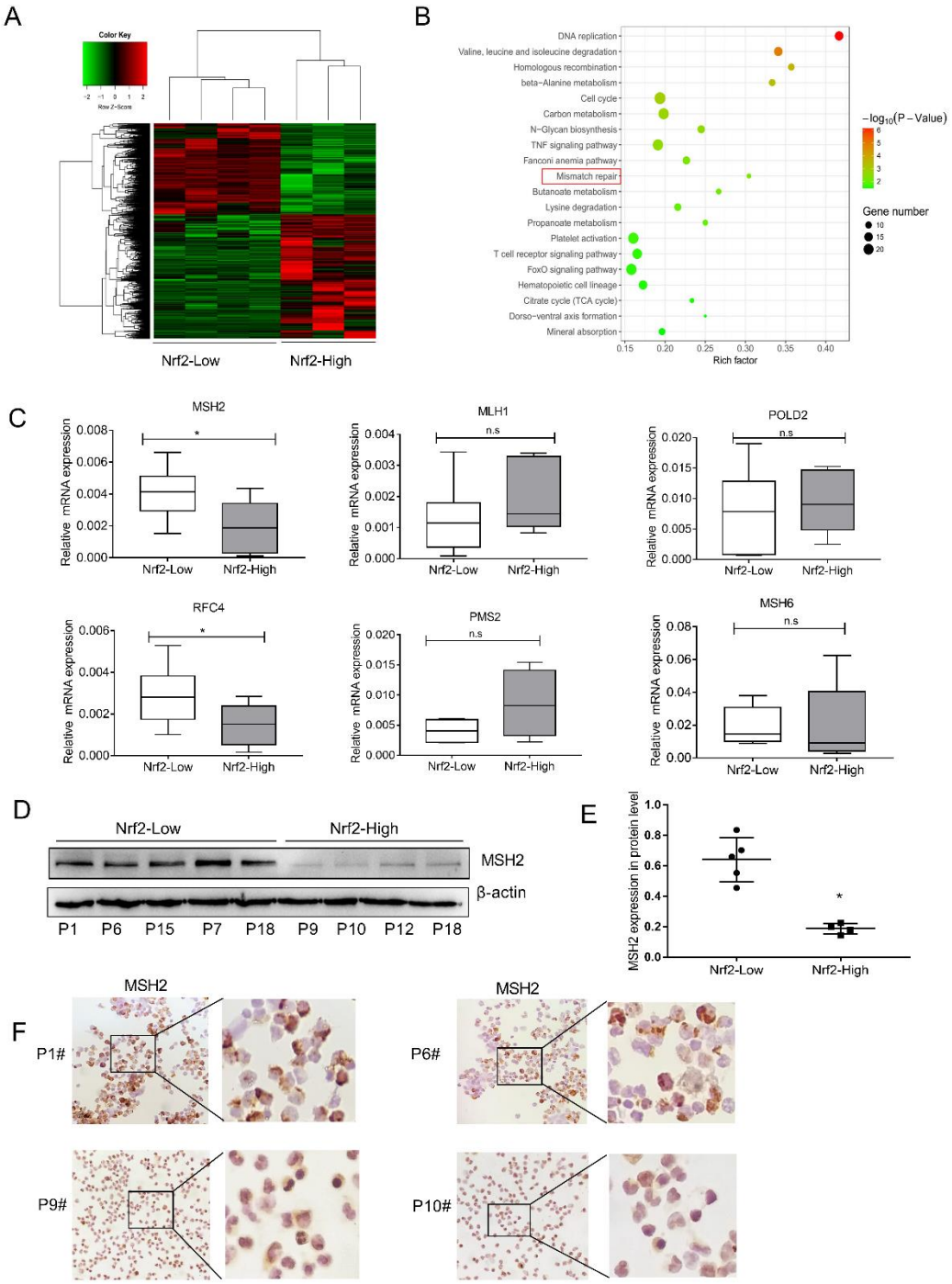


682

683 **Fig. 2** Nrf2 inhibited DNA mismatch repair pathway in AML. **a** The heatmap of
684 hierarchical clustering showed the differentially expressed genes in the Nrf2 high/low
685 expressed group based on RNAseq analysis. **b** KEGG pathway analysis showed that
686 Nrf2 expression was inhibited DNA Mismatch repair (MMR) in the AML. The KEGG
687 pathway with $P < 0.05$ was shown in a bubble plot. **c** qRT-PCR analysis of the
688 expression of the MMR genes, including MSH2, MLH1, POLD2, RFC4, PMS2 and
689 MSH6 in the Nrf2 high/low expressed group. **d** Expression levels of MSH2 protein

were detected in 9 AML samples by western blotting. **e** Quantification of MSH2 expression in Nrf2-High group and Nrf2-Ligh group. **f** Representative images of ICC staining of MSH2 in AML (P1 and P6, Nrf2-Low group; P9 and P10, Nrf2-High group), Scale bars, 50μm. Results are presented as means ± SD; *p < 0.05, **p < 0.01, ns, no significance.

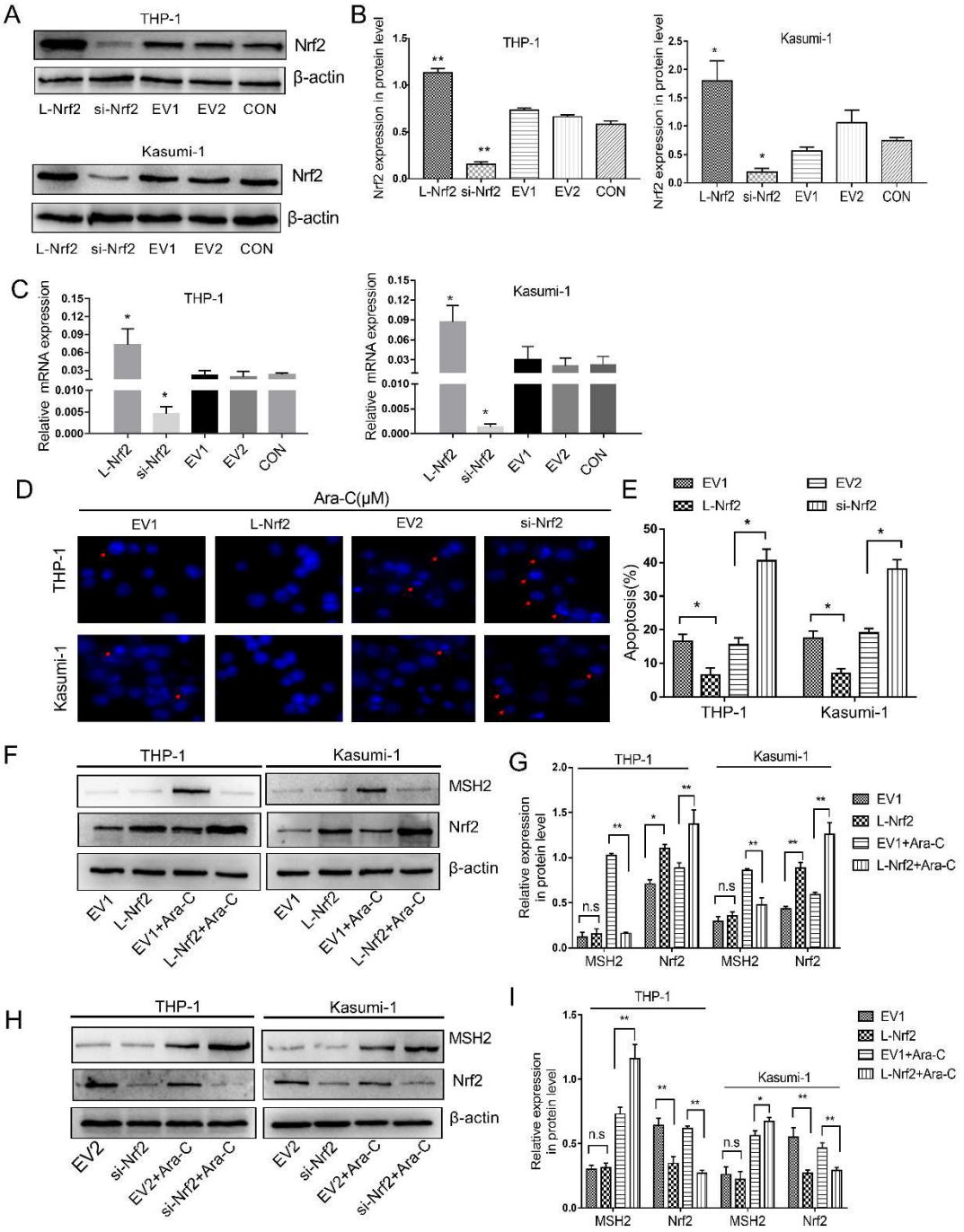


**Fig. 3** Nrf2 induced Ara-C resistance and suppressed MSH2. **a** Nrf2 was overexpressed or silenced in THP-1 and Kasumi-1 cell lines determined by western blot analyses. **b**

The relative gray values were shown in histogram. **c** Nrf2 was overexpressed or d silenced in THP-1 and Kasumi-1 cell lines determined by qRT-PCR analyses. **d, e** The necrotic cells in different groups were detected after Hoechst33342 staining (scale bars, 50 μm). **f** The Nrf2-overexpressing cells were treated with or without Ara-C (2μM) for 24 h. The Nrf2 and MSH2 protein levels were assessed by western blotting. **g** The relative gray values were shown in histogram. **h** The silencing Nrf2 cells were treated with or without Ara-C (2μM) for 24 h. The Nrf2 and MSH2 protein levels were assessed by western blotting. **i** The relative gray values were shown in histogram. Data are presented as the mean ± SD of three independent experiments. EV, empty vector. Ara-C, cytarabine. *P < 0.05, **P < 0.01, ns, no significance.

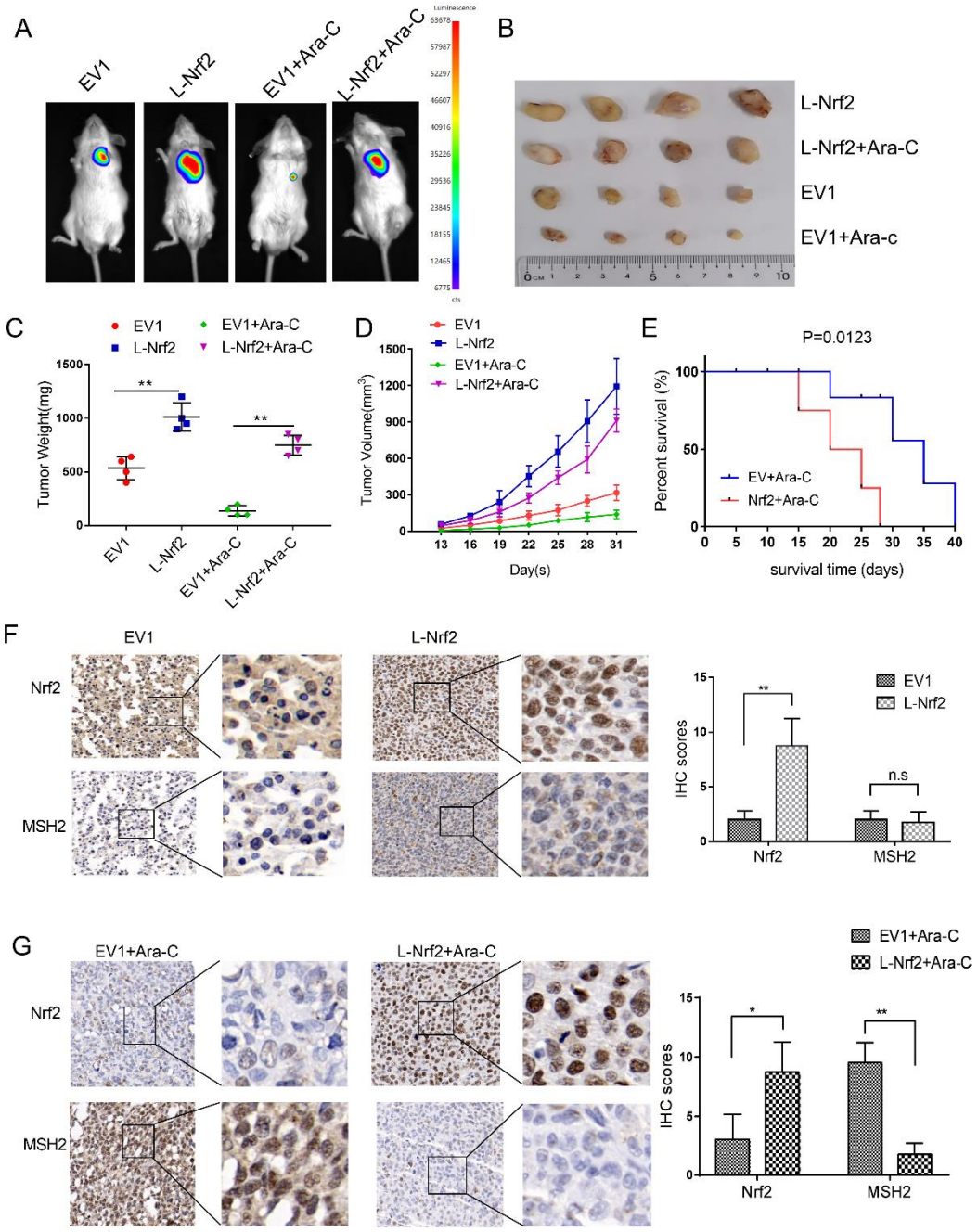


**Fig. 4** Overexpression of Nrf2 conferred higher risk of mutant drug resistance in vivo. **a** Representative images of tumor-bearing mice in the indicated cells. **b** Images of subcutaneous xenografts from mice in the EV1, L-Nrf2, EV1+Ara-C, and L-Nrf2+Ara-C groups. N = 4.**c** Tumor weight change curves for subcutaneous xenografts. **d** Tumor volume growth curves for subcutaneous xenografts. **e** Survival analysis curves for subcutaneous xenografts. Survival was plotted by using the Kaplan-Meier method. **f** The expression of Nrf2 and MSH2 was examined in xenograft tumor tissue sections using immunohistochemistry (scale bars: 50μm). *P < 0.05, **P < 0.01.

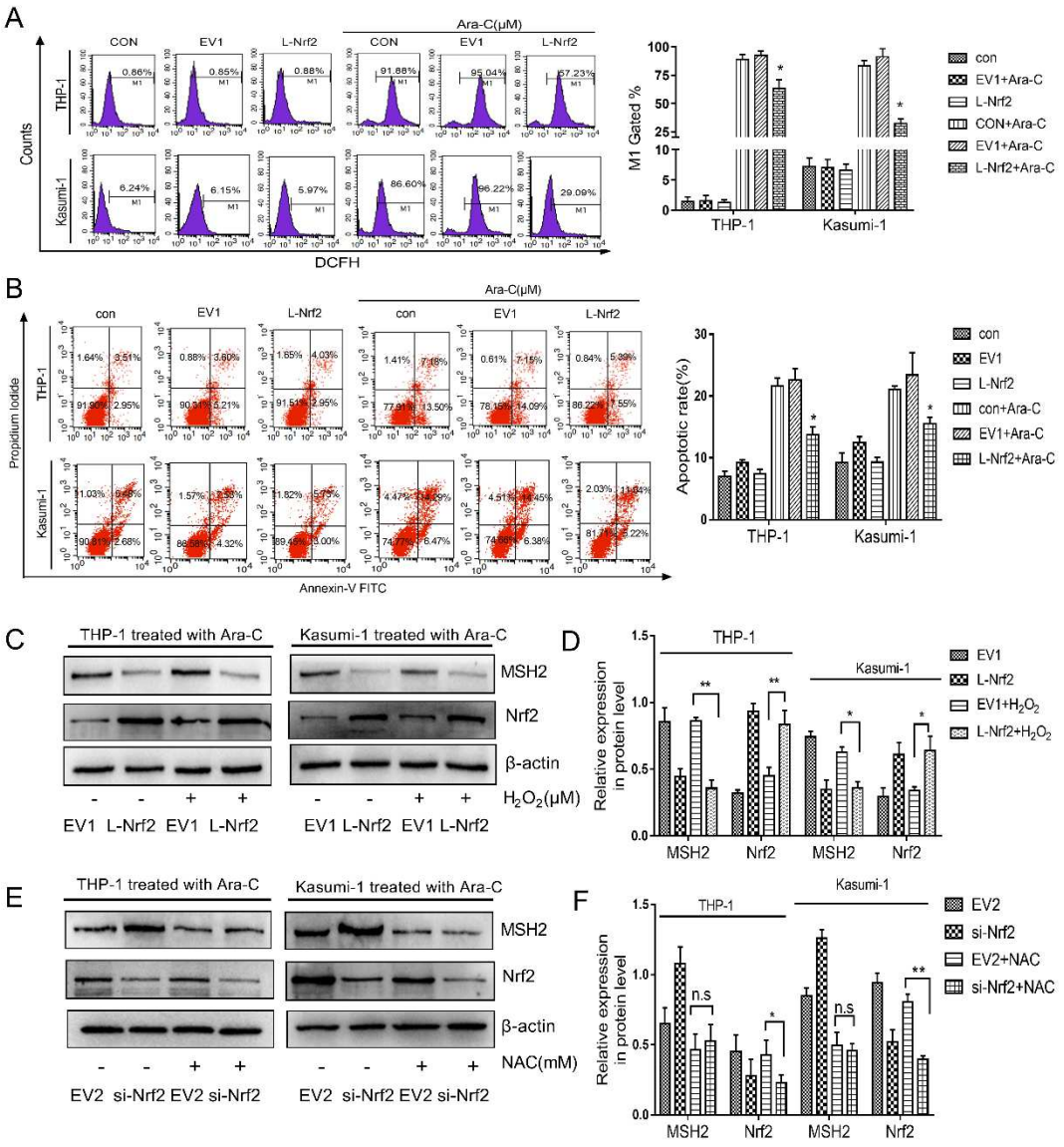


**Fig. 5** Decrease of ROS generation wasn't involved to MSH2 deregulation induced by Nrf2. **a** The cells were treated with Ara-C for 24 h. Nrf2-overexpressing and empty vector cells were stained with DCFH-DA to measure intracellular ROS production by flow cytometry. **b** The percentage of apoptotic cells was demonstrated by flow cytometry in both cell lines following the overexpression of Nrf2. **c** Nrf2-overexpressing cells were pretreated with or without $H_2O_2$ (50μM). Protein expression levels of Nrf2 and MSH2 were detected by western blotting. **d** The relative gray values were shown in histogram. **e** Silencing Nrf2 cells were pretreated with or without NAC (5mM). Protein expression levels of Nrf2 and MSH2 were detected by western blotting. **f** The relative gray values were shown in histogram. Data are presented as the mean ±

SD of three independent experiments. EV, empty vector. Ara-C, cytarabine. NAC, Nacetylcysteine. *P < 0.05, **P < 0.01, ns, no significance.

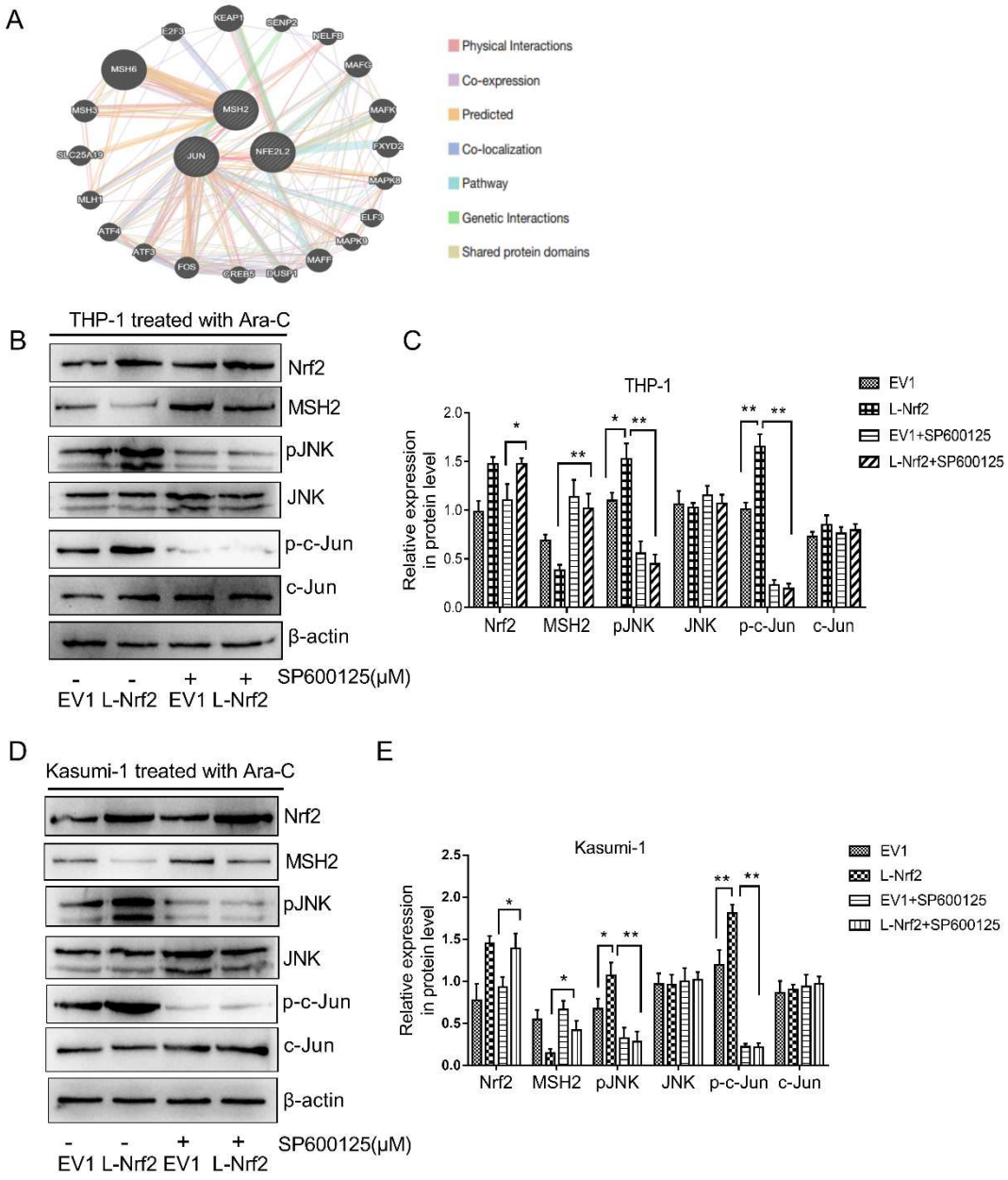


**Fig. 6** Nrf2 inhibited MSH2 through JNK/c-Jun signaling. **a** Protein-protein interaction network of Nrf2 ,MSH2 and JUN (GeneMANIA). **b** After treatment with or without 10 μM SP600125 for 24 h in THP-1 cells, protein expression levels of Nrf2, MSH2, JNK, pJNK, c-Jun and p-c-Jun was evaluated by western blot analysis in the Nrf2-overexpression and EV groups. **c** The relative gray values were shown in histogram. **d** After treatment with or without 10 μM SP600125 for 24 h in Kasumi-1 cells, protein expression levels of Nrf2, MSH2, JNK, pJNK, c-Jun and p-c-Jun was evaluated by

western blot analysis in the Nrf2-overexpression and EV groups. **e** The relative gray values were shown in histogram. Data are presented as the mean ± SD of three independent experiments. *P < 0.05, **P < 0.01, ns, no significance.

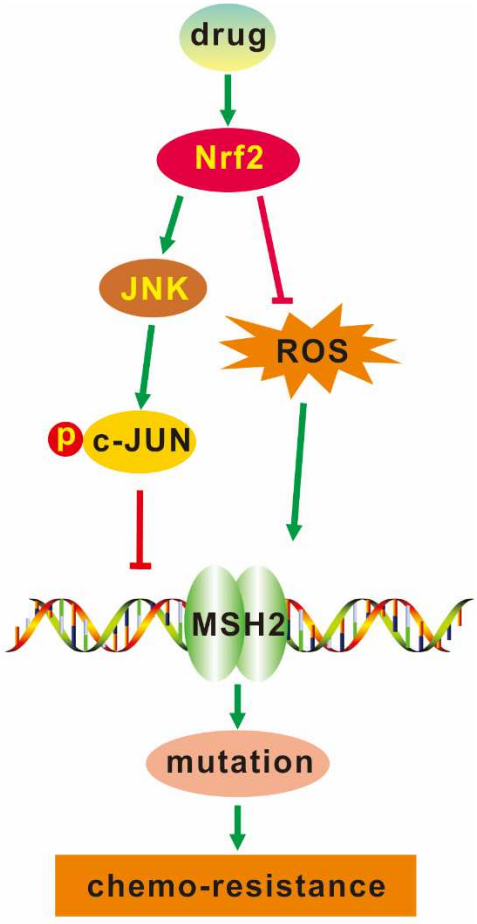


**Fig. 7** Schematic representation of Nrf2 mediated gene mutation-dependent resistance of AML cells to chemotherapy. Nrf2 reduced cytarabine-induced ROS and positively regulated JNK, activating the phosphorylated c-Jun, leading to inhibition of DNA MMR and finally mutation-dependent resistance.

752 **Figure S1A, B**

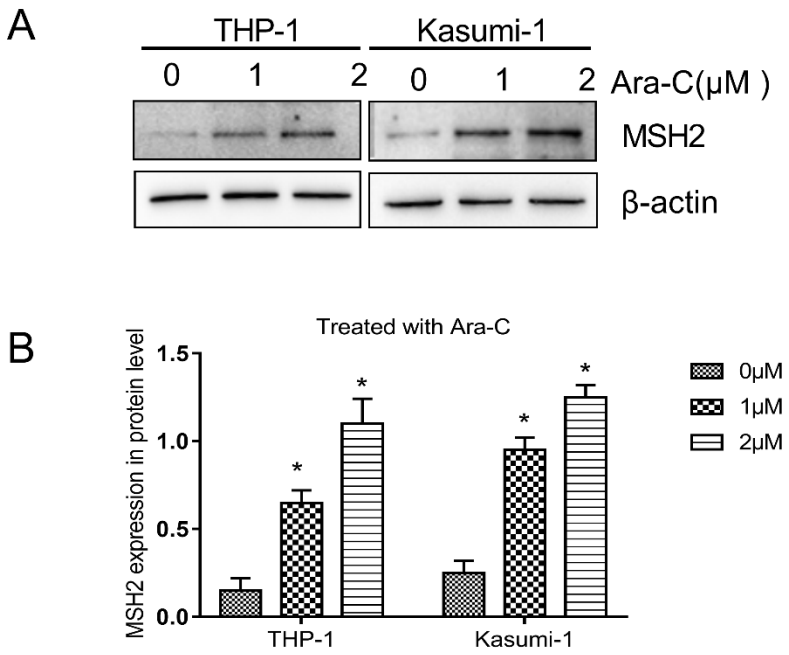


753

754 Figure S1. (a) The MSH2 protein levels were accumulated during exposure to Ara-C in
755 THP-1 and Kasumi-1 cells assessed by western blot and (b) the relative gray values
756 were shown in histogram

757

# Figures

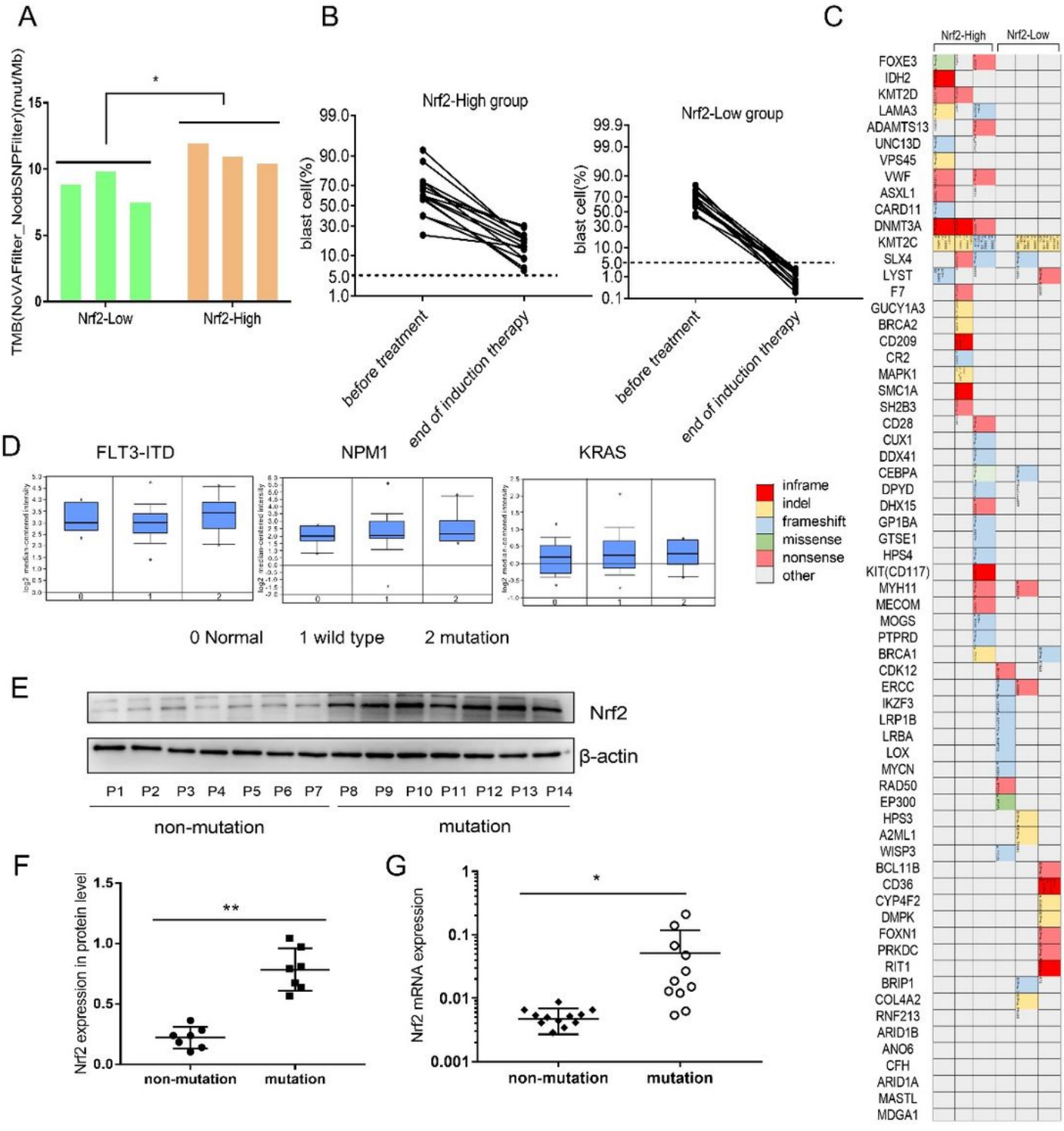


**Figure 1**

Nrf2 expression and tumor mutation burden in AML. a TMB values of mutation sites in Nrf2 high/low expression group. b The percentage of blast cells were detected in 15 matched Nrf2 high/low AML specimens. c Disease-related gene mutations were shown in AML patients with high/low expression of

Nrf2 by whole-exon sequencing. d Studies in the Oncomine database showed higher mRNA expression of Nrf2 in AML patients with FLT3-ITD, NPM1, KRAS positive mutations. e Expression levels of Nrf2 protein were detected in 14 AML specimens by western blotting (P: patient). f Quantification of Nrf2 expression in AML samples. g mRNA expression of Nrf2 in AML by qRT-PCR. Results are presented as means ± SD; TMB, tumor mutation burden. *p < 0.05, **p < 0.01.

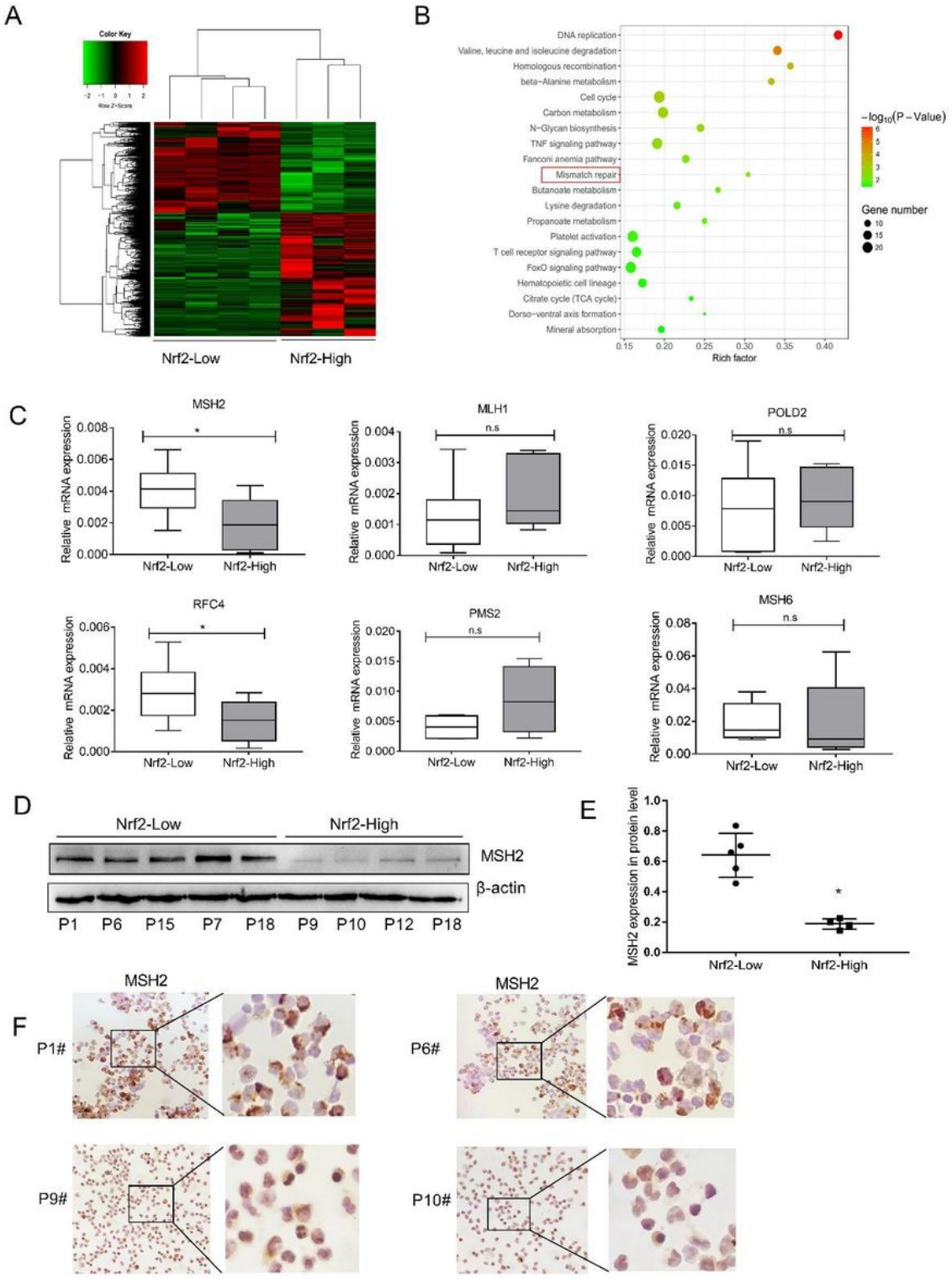


Figure 2

Nrf2 inhibited DNA mismatch repair pathway in AML. a The heatmap of hierarchical clustering showed the differentially expressed genes in the Nrf2 high/low expressed group based on RNAseq analysis. b KEGG pathway analysis showed that Nrf2 expression was inhibited DNA Mismatch repair (MMR) in the AML. The KEGG pathway with $P < 0.05$ was shown in a bubble plot. c qRT-PCR analysis of the expression of the MMR genes, including MSH2, MLH1, POLD2, RFC4, PMS2 and MSH6 in the Nrf2 high/low expressed group. d Expression levels of MSH2 protein were detected in 9 AML samples by western blotting. e Quantification of MSH2 expression in Nrf2-High group and Nrf2-Ligh group. f Representative images of ICCstaining of MSH2 in AML (P1 and P6, Nrf2-Low group; P9 and P10, Nrf2-High group), Scale bars, 50μm. Results are presented as means ± SD; *$p < 0.05$, **$p < 0.01$, ns, no significance.

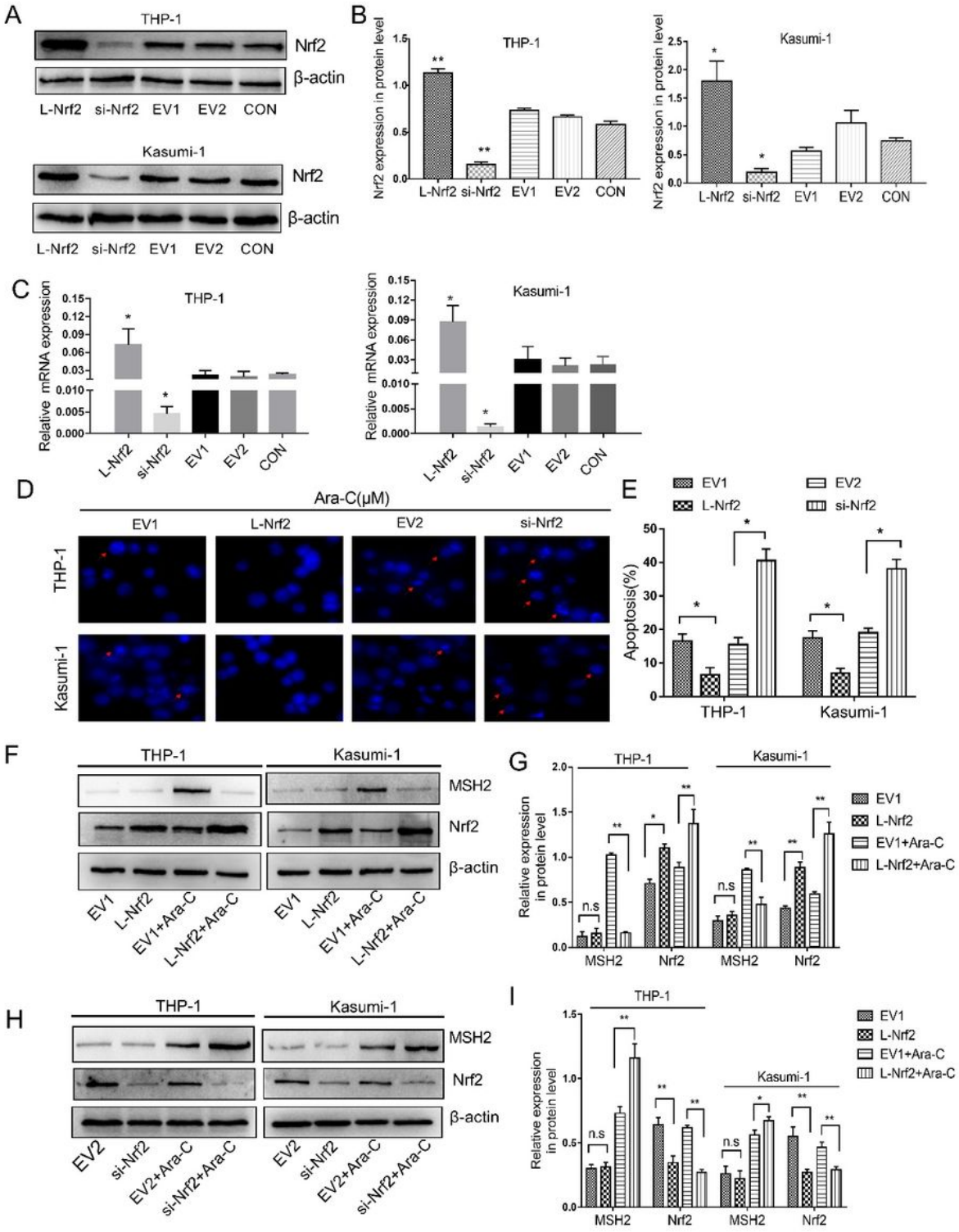


## Figure 3

Nrf2 induced Ara-C resistance and suppressed MSH2. a Nrf2 was overexpressed or silenced in THP-1 and Kasumi-1 cell lines determined by western blot analyses. b The relative gray values were shown in histogram. c Nrf2 was overexpressed or d silenced in THP-1 and Kasumi-1 cell lines determined by qRT-PCR analyses. d, e The necrotic cells in different groups were detected after Hoechst33342 staining (scale bars, 50 μm). f The Nrf2-overexpressing cells were treated with or without Ara-C (2μM) for 24 h. The Nrf2

and MSH2 protein levels were assessed by western blotting. g Therelative gray values were shown in histogram. h The silencing Nrf2 cells were treated with or without Ara-C (2μM) for 24 h. The Nrf2 and MSH2 protein levels were assessed by western blotting. i The relative gray values were shown in histogram. Data are presented as the mean ± SD of three independent experiments. EV, empty vector. Ara-C, cytarabine. *P < 0.05, **P < 0.01, ns, no significance.

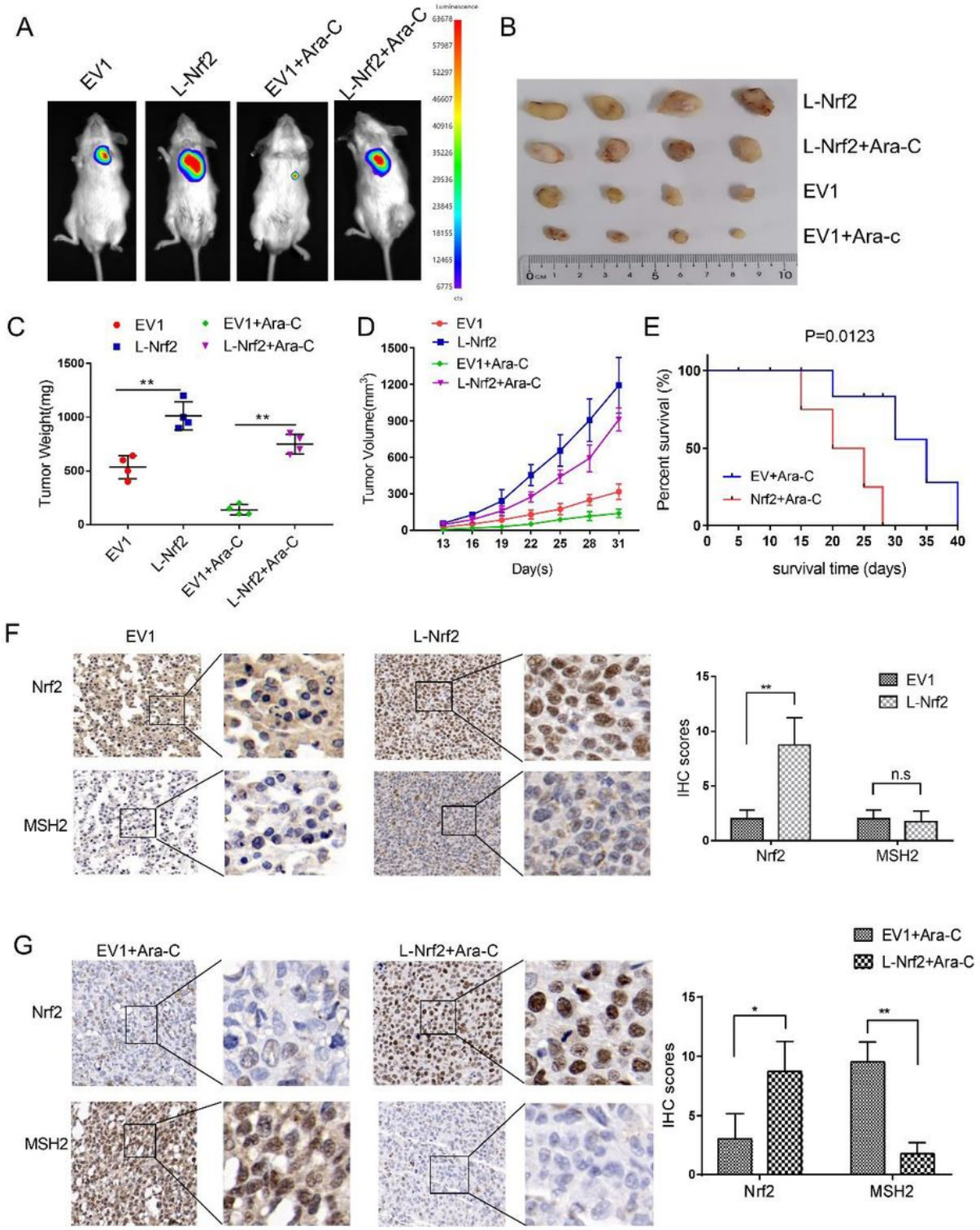


Figure 4

Overexpression of Nrf2 conferred higher risk of mutant drug resistance in vivo. a Representative images of tumor-bearing mice in the indicated cells. b Images of subcutaneous xenografts from mice in the EV1, L-Nrf2, EV1+Ara-C, and L-Nrf2+Ara-C groups. N = 4.c Tumor weight change curves for subcutaneous xenografts. d Tumor volume growth curves for subcutaneous xenografts. e Survival analysis curves for subcutaneous xenografts. Survival was plotted by using the Kaplan-Meier method. f The expression of Nrf2 and MSH2 was examined in xenograft tumor tissue sections using immunohistochemistry (scale bars: 50μm). *P < 0.05, **P < 0.01.

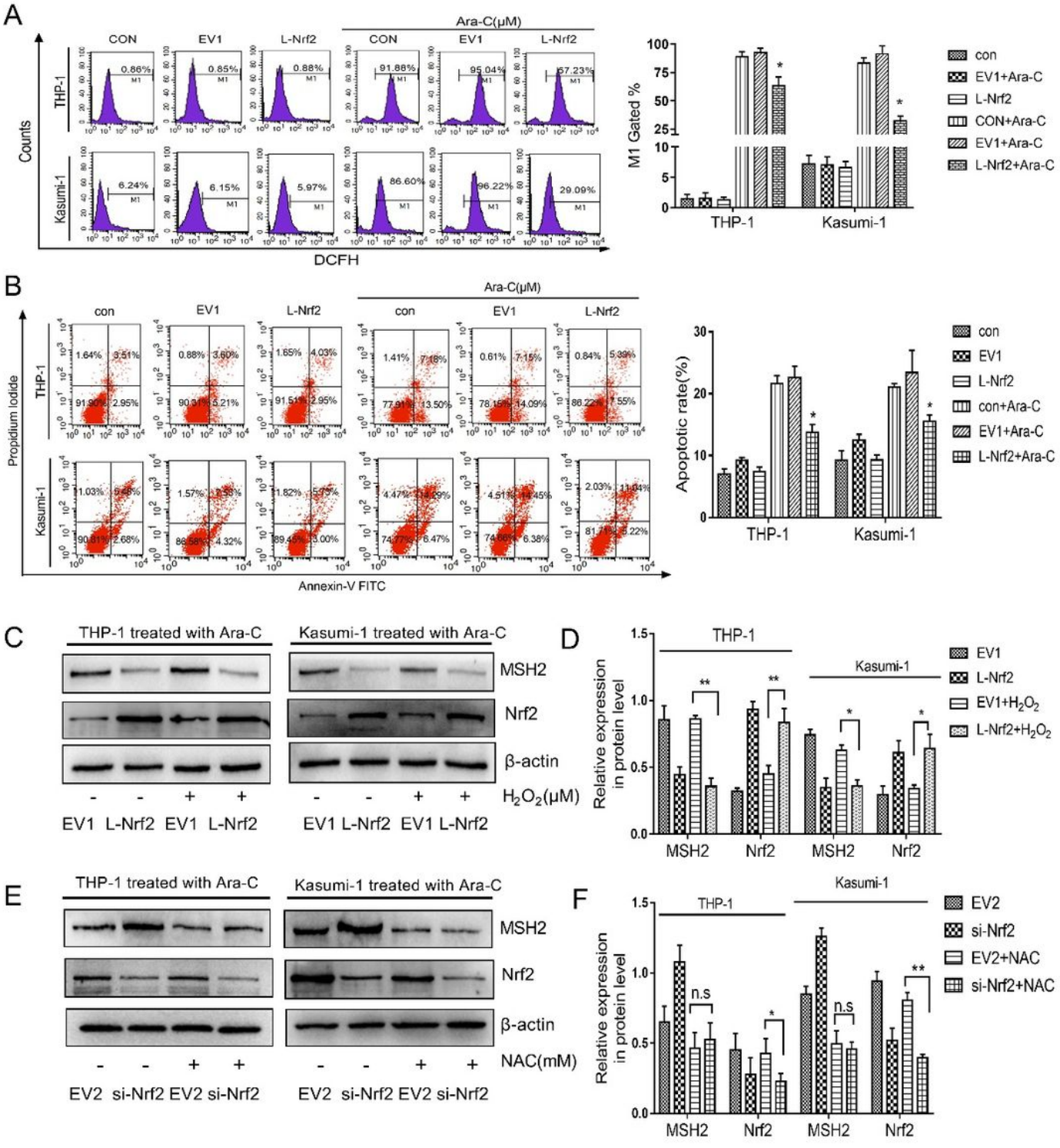

## Figure 5

Decrease of ROS generation wasn't involved to MSH2 deregulation induced by Nrf2. a The cells were treated with Ara-C for 24 h. Nrf2-overexpressing and empty vector cells were stained with DCFH-DA to measure intracellular ROS production byflow cytometry. b The percentage of apoptotic cells was demonstrated by flow cytometry in both cell lines following the overexpression of Nrf2. c Nrf2-overexpressing cells were pretreated with or without H2O2 (50μM). Protein expression levels of Nrf2 and MSH2 were detected by western blotting. d The relative gray values were shown in histogram. e Silencing Nrf2 cells were pretreated with or without NAC (5mM). Protein expression levels of Nrf2 and MSH2 were detected by western blotting. f The relative gray values were shown in histogram. Data are presented as the mean ± SD of three independent experiments. EV, empty vector. Ara-C, cytarabine. NAC, Nacetylcysteine. *P < 0.05, **P < 0.01, ns, no significance.

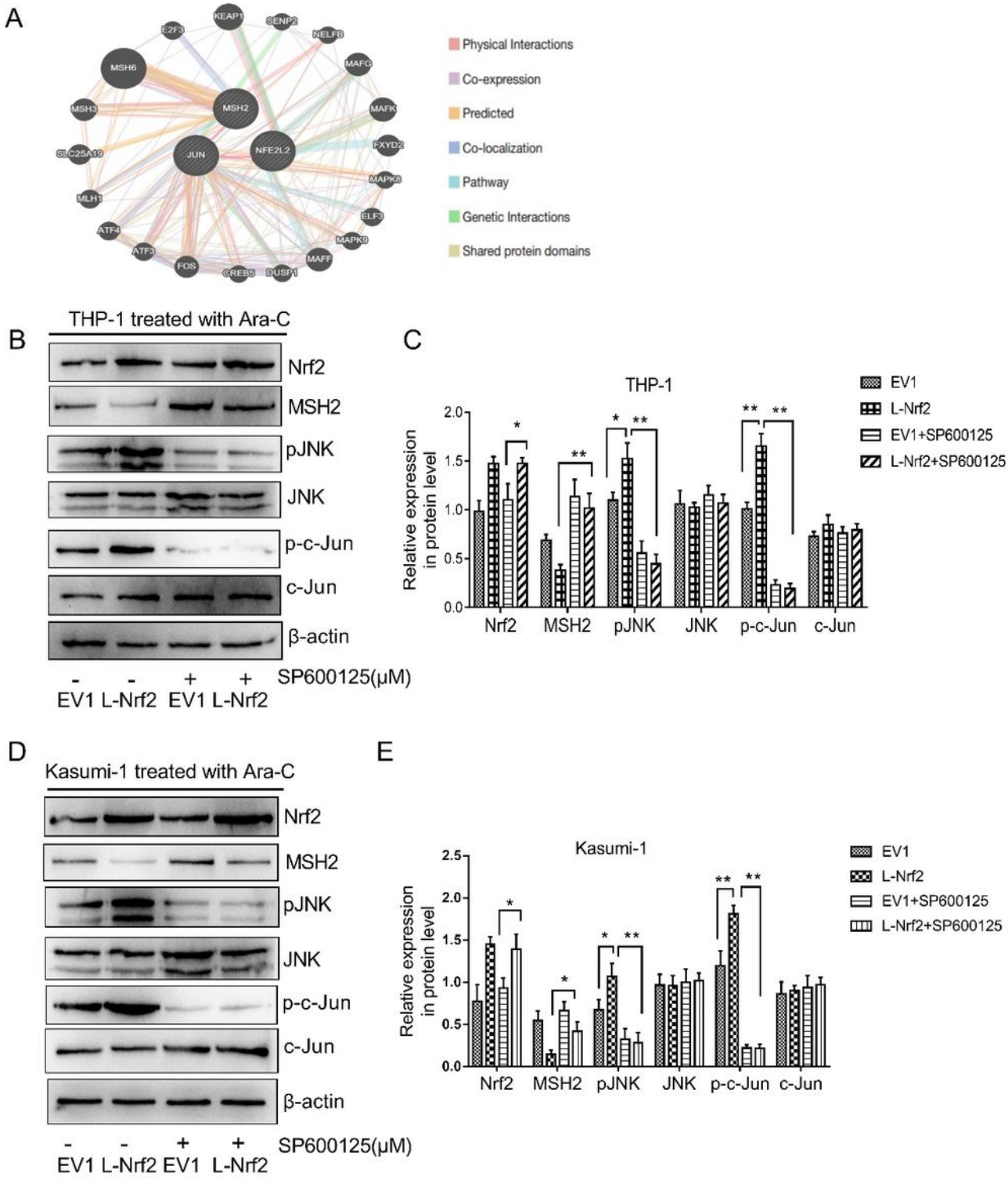


## Figure 6

Nrf2 inhibited MSH2 through JNK/c-Jun signaling. a Protein-protein interaction network of Nrf2 ,MSH2 and JUN (GeneMANIA). b After treatment with or without 10 μM SP600125 for 24 h in THP-1 cells, protein expression levels of Nrf2, MSH2, JNK, pJNK, c-Jun and p-c-Jun was evaluated by western blot analysis in the Nrf2- overexpression and EV groups. c The relative gray values were shown in histogram. d After treatment with or without 10 μM SP600125 for 24 h in Kasumi-1 cells, protein expression levels of Nrf2,

MSH2, JNK, pJNK, c-Jun and p-c-Jun was evaluated by western blot analysis in the Nrf2-overexpression and EV groups. e The relative gray values were shown in histogram. Data are presented as the mean ± SD of three independent experiments. *P < 0.05, **P < 0.01, ns, no significance.

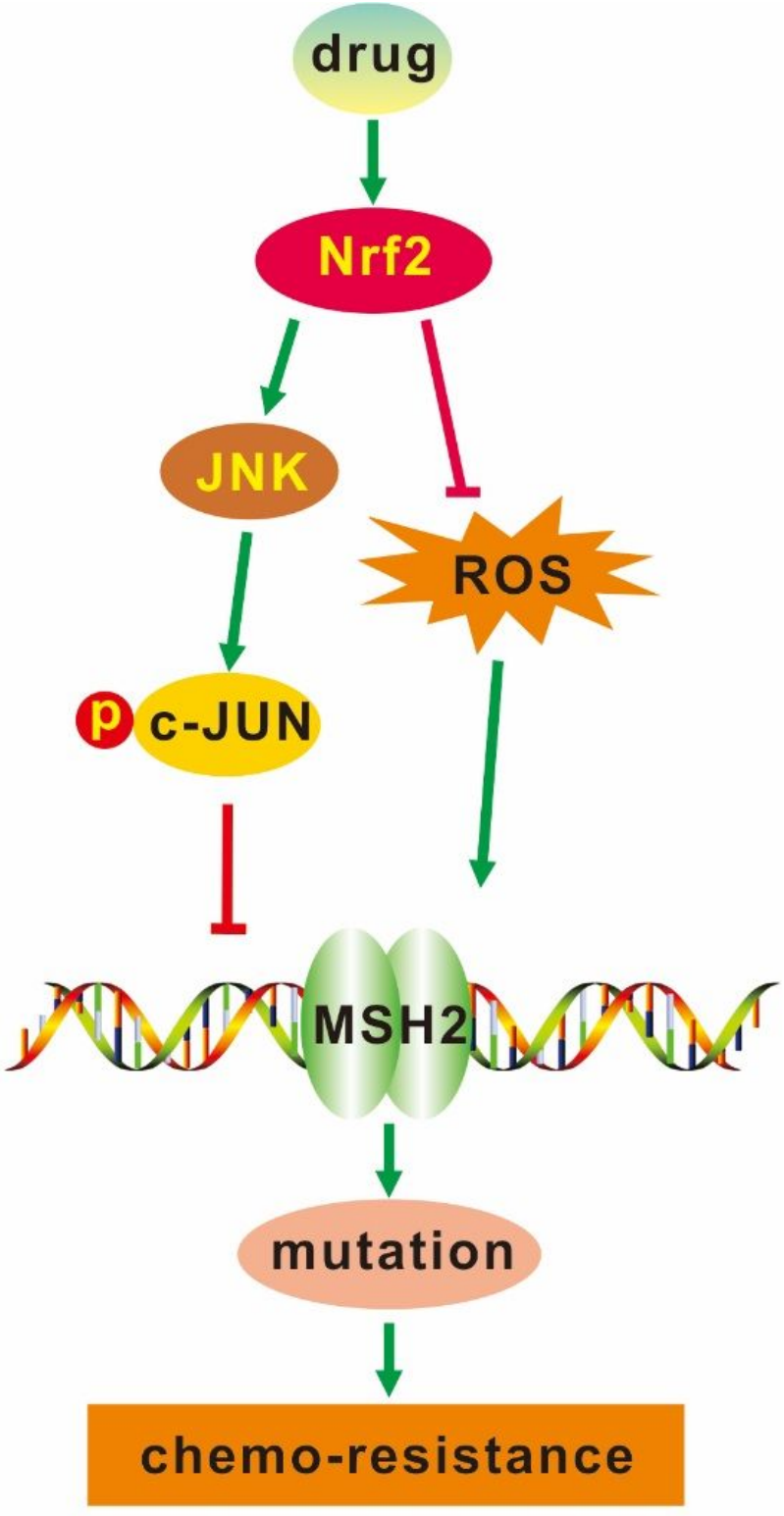


**Figure 7**

Schematic representation of Nrf2 mediated gene mutation-dependent resistance of AML cells to chemotherapy. Nrf2 reduced cytarabine-induced ROS and positively regulated JNK, activating the

phosphorylated c-Jun, leading to inhibition of DNA MMR and finally mutation-dependent resistance.

## Supplementary Files

This is a list of supplementary files associated with this preprint. Click to download.

- FigureS1AB.tif
- FigureS1AB.tif
- Table.pdf
- Table.pdf